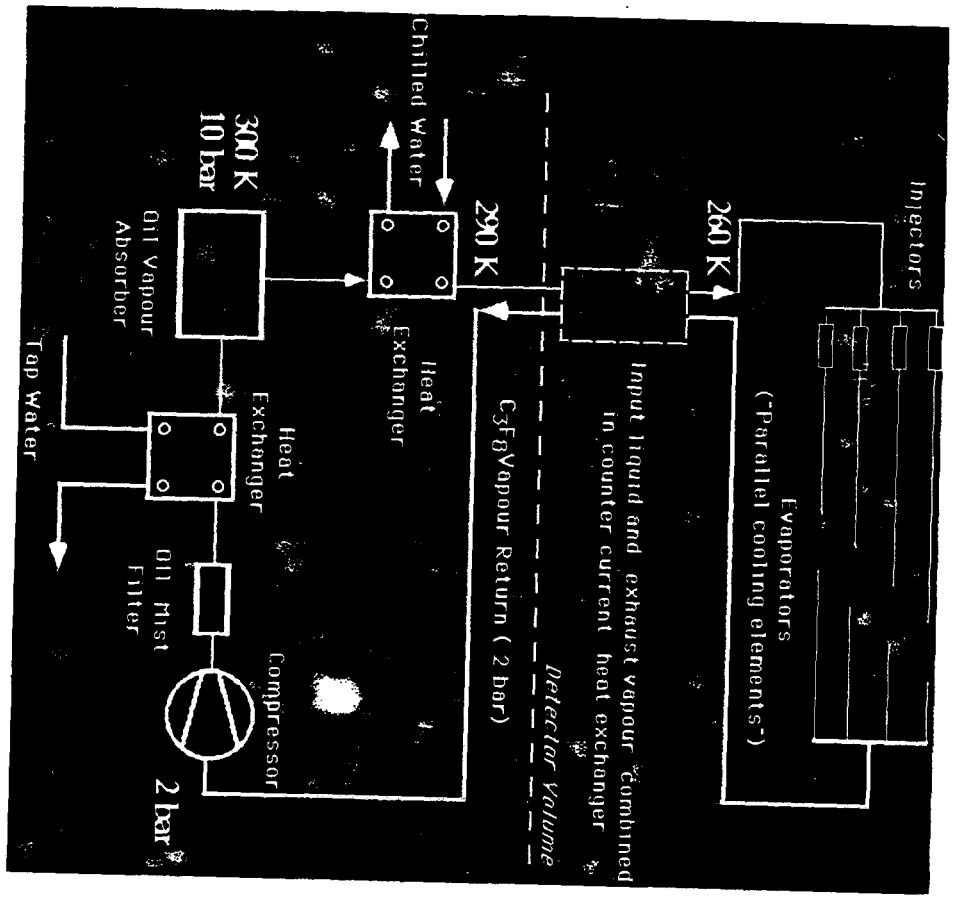

P ressure-Enthalpy Chart for PF-5030

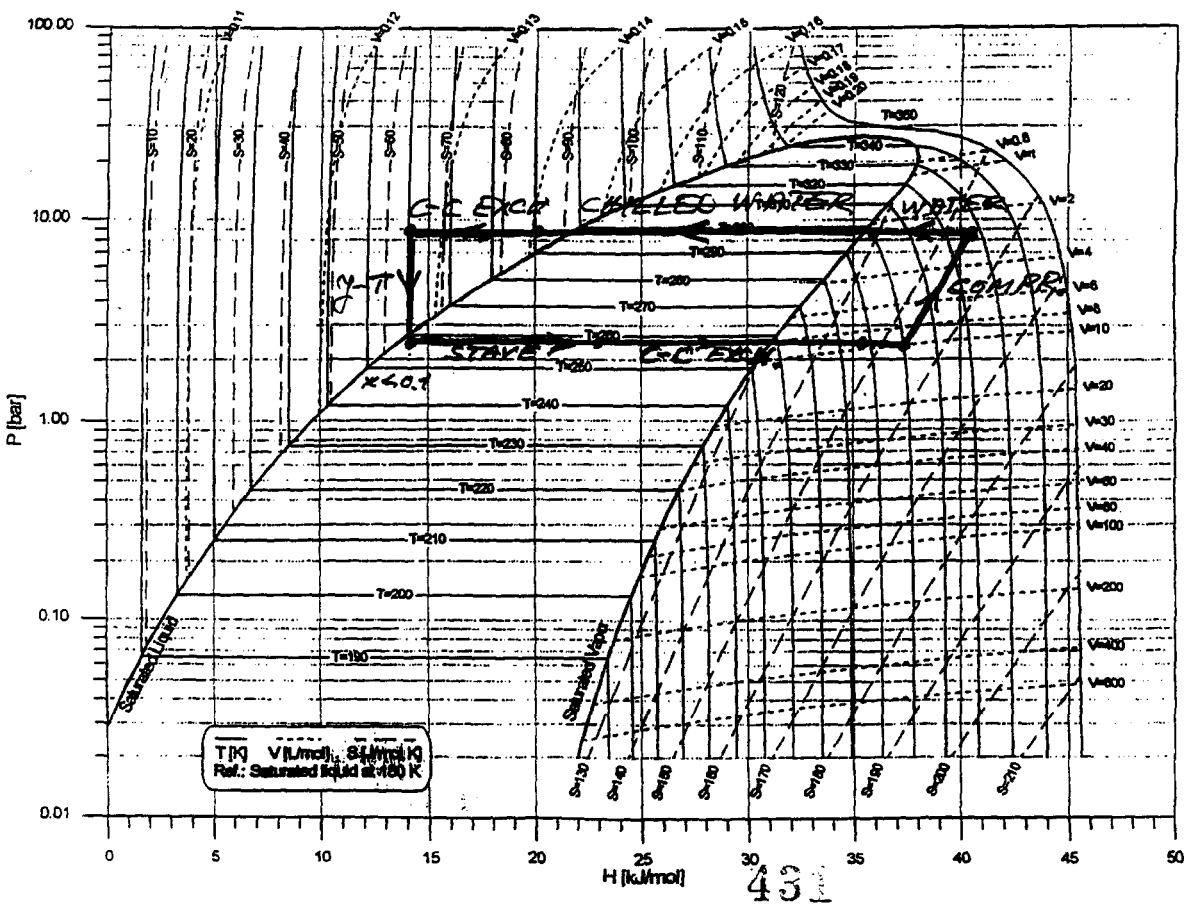

EVAPORATIVE COOLING WITH C_4F_{10} FLUOROCARBON HAS BEEN SUCCESFUL WITH ALL ATLAS PIXEL STRUCTURES SO FAR TESTED.

C_4F_{10} EVAPORATION GIVES COOLING TUBE WORKING PRESSURES AROUND 500 mbar (abs) FOR TEMPERATURES AROUND $-10°C$ (S.V.P. CURVE). ALLOWING USE OF THIN WALL (LOW X/X_0) TUBE ACROSS DETECTOR ACTIVE AREA.

ONLY PART OF SYSTEM

INJECTORS CAN BE VERY SMALL, ROBUST, ACCURATELY MATCHED AND INEXPENSIVE: RUBY WATCH JEWELS

TESTS WILL CONTINUE IN ATLAS WITH NEW PIXEL STRUCTURES AND WITH STRUCTURES FROM THE BARREL AND FORWARD SCT.

ATLAS Pixel Disk Mechanics

E. Anderssen, D. Bintinger, J. Emes, M. Gilchriese,
F. McCormack
Lawrence Berkeley National laboratory

W. O. Miller
HYTEC Inc.

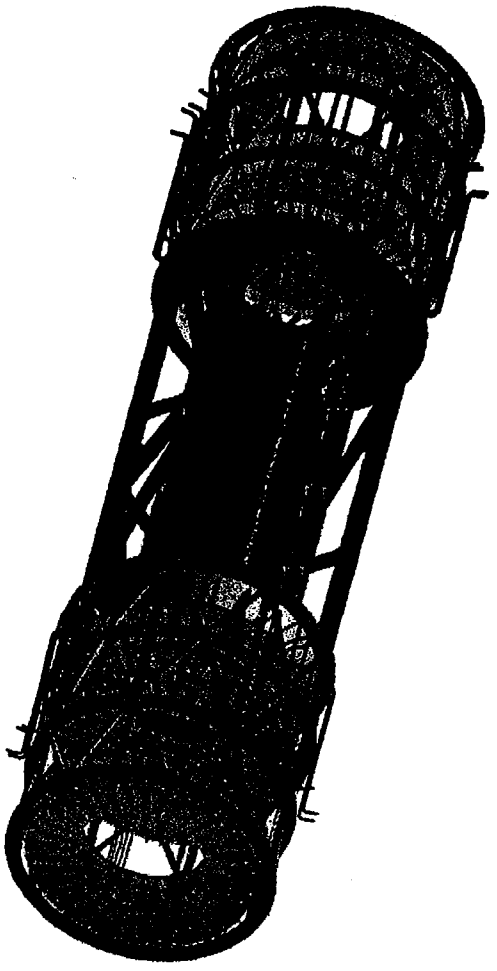

Disk Layout Considerations

Modules arrayed on both sides of disk for complete coverage

Leads to: Balanced mechanical structure

Reduced heat flux into coolant flow

Provide cooling over entire active area ~ 400 W/disk

Desire similar disk and barrel modules

Divide disks into sectors ~ 12 sectors/disk
As alignment units
cooling units
assembly units

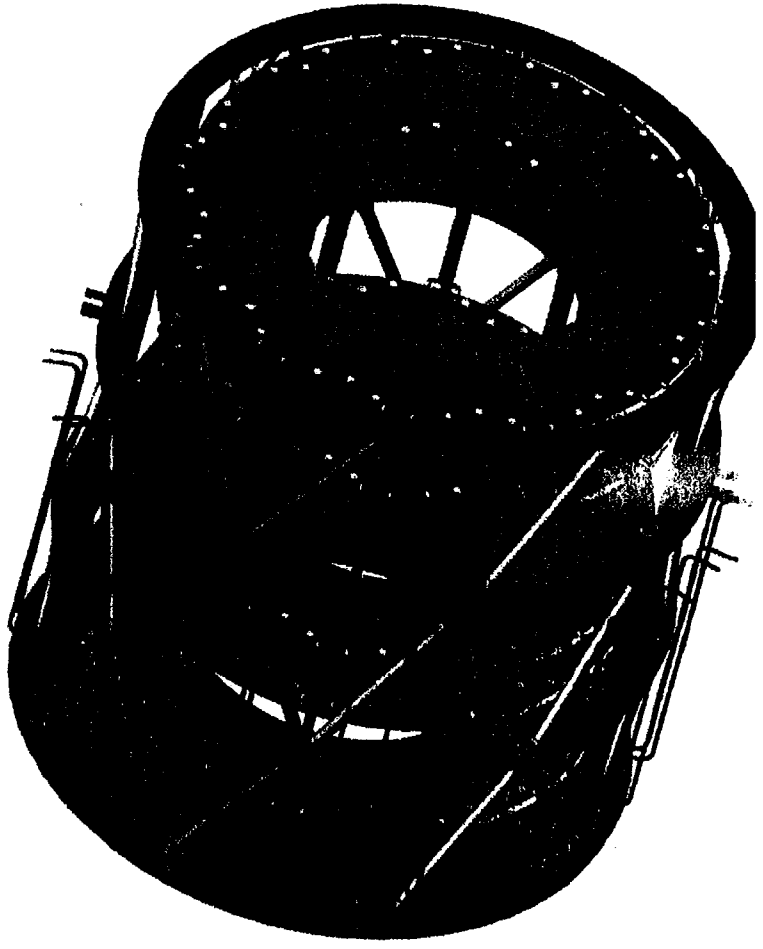

Pixel Disk Mechanical Design

Basic design unit is the Sector.

A sandwich design for a sector is natural given layout:
- Stiff, heat conducting, low CTE Face Plates
- Shaped Cooling Tube between face plates
- Fill of minimal mass

Face Plates: investigated aluminum, beryllium, albemet, CFR composites, Carbon-Carbon, graphites, etc.
- Have chosen Carbon-Carbon:
  - CTE xy: -1.0 ppm/K, z: 6.0 ppm/K
  - Modulus ~ 185 GPa
  - Thermal conductivity ~ xy: 200 W/mK, z: 32 W/mK
  - Radiation length 23 cm
  - Nonhygroscopic

Cooling Tube: investigating glassy carbon, sealed carbon-carbon, sealed graphite, and aluminum
- No decision at present. Prototypes underway.

Interfacing Fill: investgating carbon fibers (with glassy carbon tube) and reticulated vitreous carbon
- No decision at present. Prototypes underway.

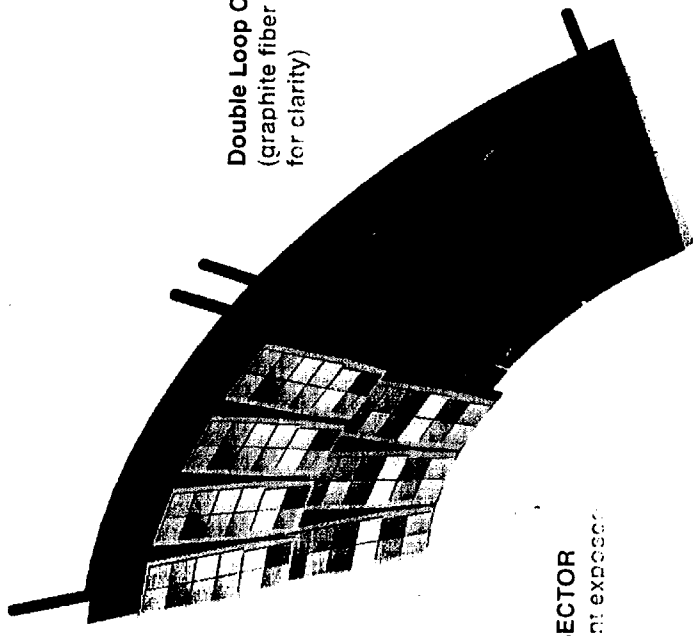

Pixel Disk Sector Prototype Programs

Prototype program 1: Carbon-carbon facings (0.5 mm thick), shaped glassy carbon coolant tube (3.2 mm id), high thermal conductivity carbon fiber fill (goal 5% density).

Prototypes constructed by Energy Science Laboratories, Inc. (ESLI). ESLI has succeeded in fabricating shaped glassy carbon tubes of appropriate ID and wall thickness.

Prototypes 4 and 6 have average radiation lengths of 0.73% and 0.65% respectively.

Prototype 4 is currently undergoing ESPI testing.

Main concern is thermal connection via fibers between coolant tube and facings.

Prototype program 2: Carbon-carbon facings (0.5 mm thick), shaped and flattened aluminum coolant tube (3.6 mm id, 0.2 mm wall), and reticulated vitreous carbon fill (3% density).

Have succeeded in shaping 0.2 mm wall aluminum tube.

Prototype 3 has average radiation length of 0.76%.

Prototype 2 showed good structural characteristics in ESPI tests without dummy silicon modules.

Prototype 3 has shown excellent thermal characteristics with water based coolant.

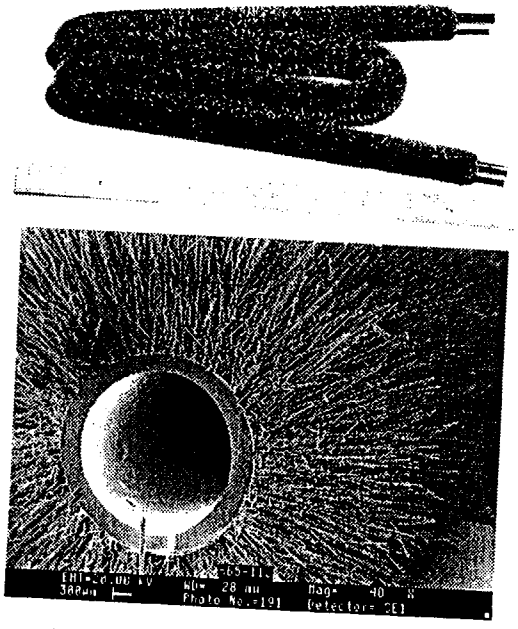

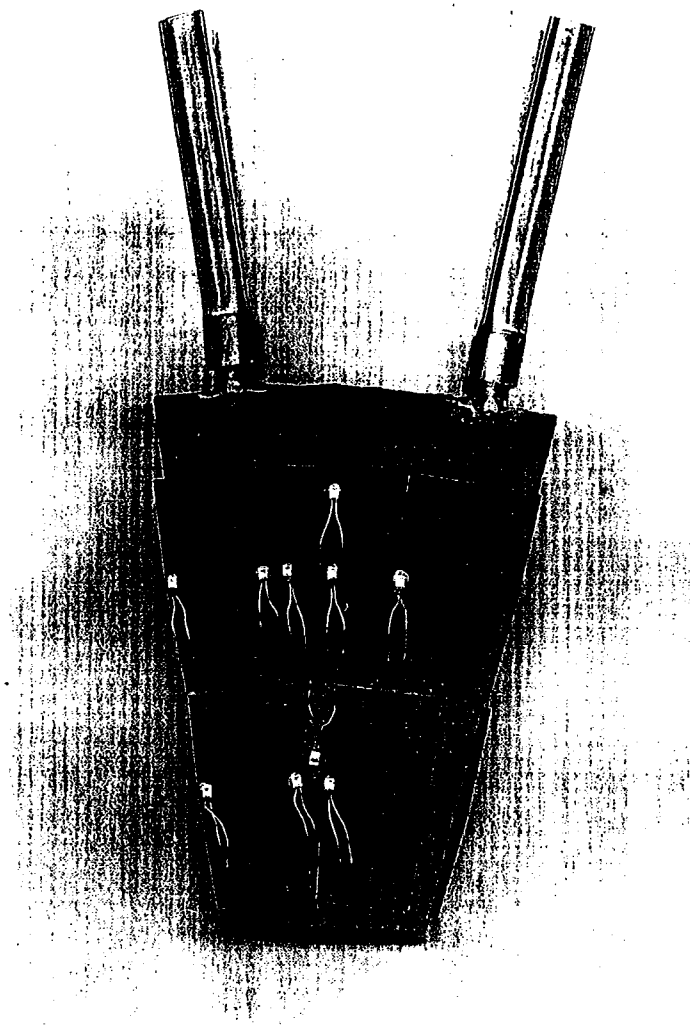

ESL1 Sector 4

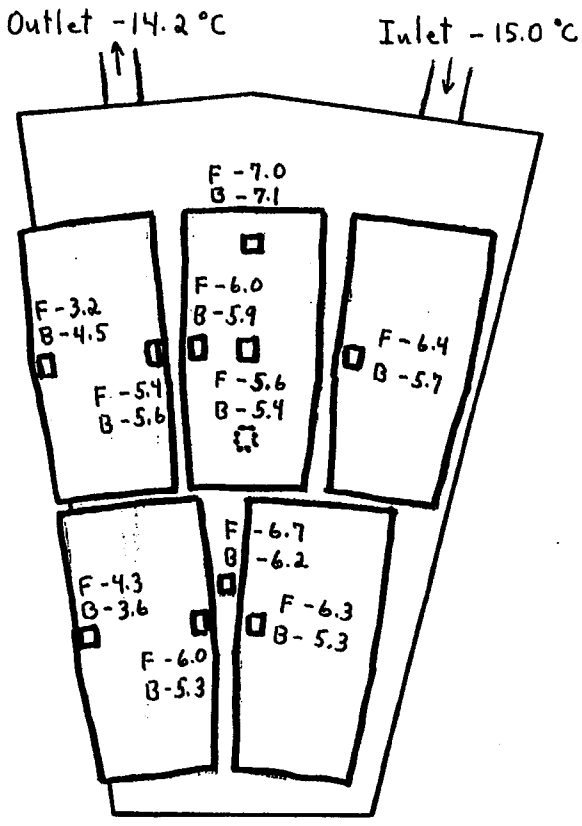

Coolant: 30% Methanol by volume
Flow: 11.8 cc/sec , Δp = 208 mb
Adhesive for Silicon: 125μ of CGL7018
Power: 36W , Ambient - 8.7°C

Title:
Sub-region size: 752,576 Layer: 1 Scaling factor: 0.5 Range: 2,20 Current date: 22-May-1997 Current time: 10:10:54

Pixel Mechanics Meeting

ESLI Sector #3
0.96 °C ΔT T₁ = 6.14 °C No Heater Pwr Coolant 1.7 cc/s
"Bear Paw" Pattern 4 Fringes over wafer region 1.04 μm's
2 Fringes along sides, some at bottom ~ 1.3 μm's

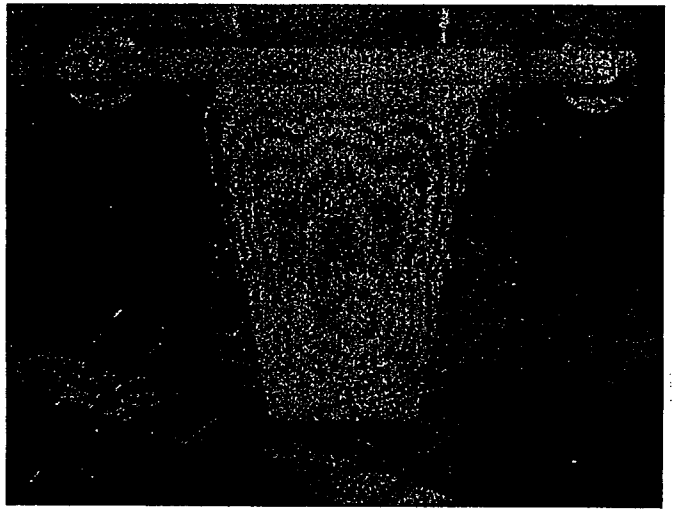

21/May/1997 ESLI #3 1630-1640

Picture size: 752,576,1 Class: Image Form: Byte Creation date: 27-Apr-1998 Creation time: 16:15:42
Title:
Sub-region size: 752,576 Layer: 1 Scaling factor: 0.5 Range: 1,10 Current date: 27-Apr-1998 Current time: 16:16:02

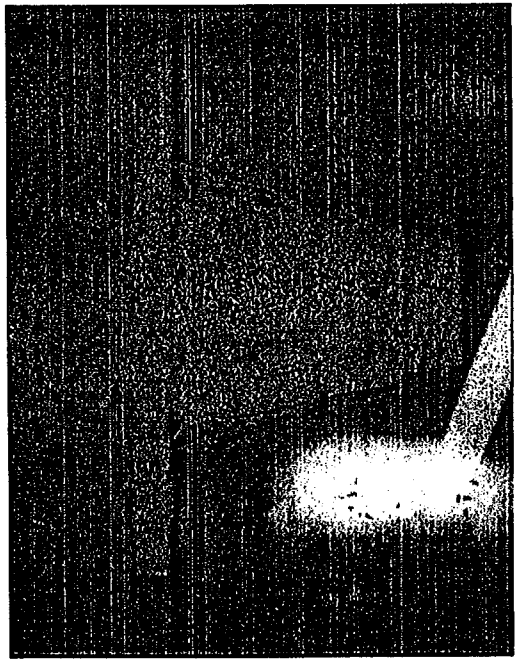

27 Apr 2:14-2:16 -7.0 to -11.0 C

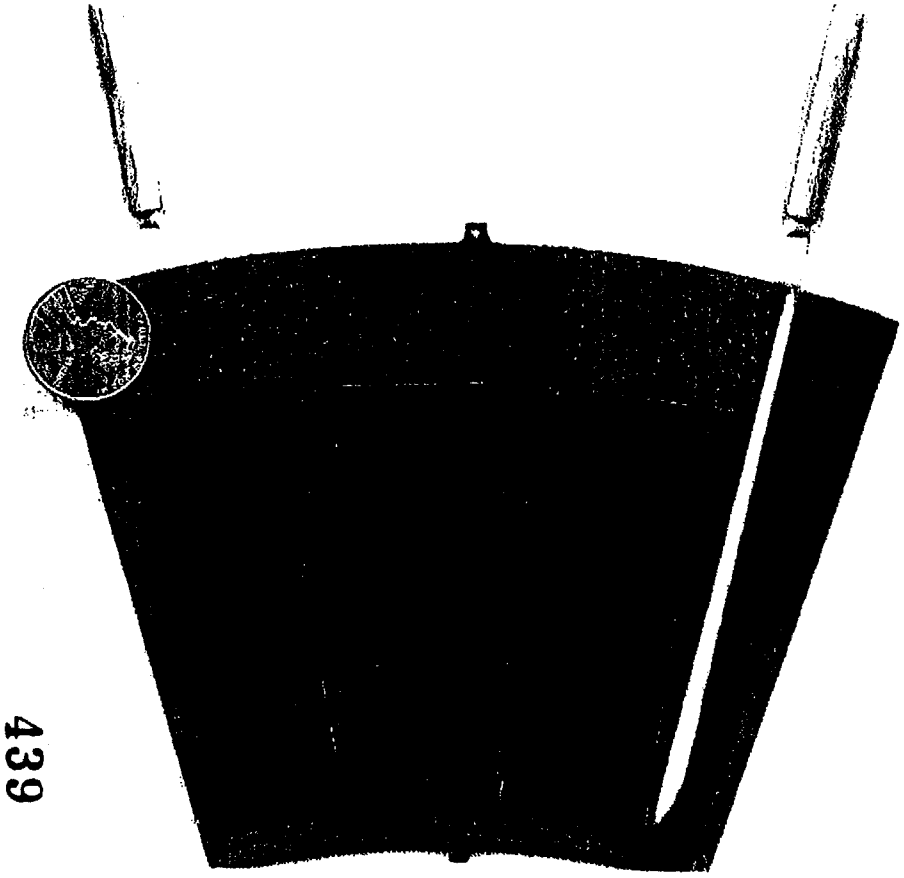

RETICULATED VITREOUS CARBON (RVC)*

WHAT IS RVC?

RVC is a new open pore foam material composed solely of vitreous carbon. Vitreous carbon, as the name implies, is a form of glass-like carbon which combines some of the properties of glass with some of those of normal industrial carbons. RVC has an exceptionally high void volume (97%), high surface area combined with self-supporting rigidity, low resistance to fluid flow, and resistance to very high temperatures in non-oxidizing environments. It is now available in a wide range of pore size grades weighing about 3 pounds per cubic foot.

WHAT IS DISTINCTIVE ABOUT RVC?

- Exceptional chemical inertness over a very wide temperature range.
- Unique high-temperature strength combined with low bulk thermal conductivity.
- Unusual rigid geometry which provides a large surface area combined with low pressure drop to fluid flow, along with great ability to hold infused materials within controlled porosity sizes.
- Electrical conductivity.

HOW CAN RVC BE USED?

- Porous Electrodes—for electrochemical processes that require very high current distribution areas, low electrical or fluid flow resistance, and minimal cell volume loss to electrodes.
- High Temperature Insulation—for inert gas and vacuum furnaces where its ease of fabrication, self-supporting nature, low density, low outgassing, low heat capacity and excellent K value combine to improve efficiency and reduce costs over conventional insulating materials.
- Filters and Demisters—for molten metals, corrosive chemicals, high or low temperature gases and liquids, where maximum chemical inertness combined with good filtration and detrainment is needed.
- Storage Batteries—in high energy density batteries, such as the sodium/sulfur and lithium aluminum/iron disulfide systems, where its unique "caging" effect on infused materials benefits performance, reduces cost.
- Scaffolds—for biological growth (it is non-toxic and biologically inert) in pollution-control systems, as a catalyst or catalyst support, in tower packings, where low pressure drop combined with large available surface area and chemical inertness is required.
- Semi-Conductor Manufacture—offers unique advantages in etching and diffusion treatment carriers, reduces manufacturing cost.
- Acoustic Control—a specially densified form combines outstanding high temperature resistance in non-oxidizing environments with excellent noise absorption in the 250 Hz to 3 kHz range.

WHAT ARE RVC'S PROPERTIES?

CHEMICAL PROPERTIES

RVC is composed of one of the most chemically inert forms of carbon known. Its oxidation resistance is unusual for a carbon. In spite of RVC's large surface area it does not support combustion after heating to bright incandescence in air followed by removal of the heat source. It is also highly resistant to intercalation by materials which disintegrate graphite.

RVC is also inert to a wide range of very reactive acids, bases, and organic solvents. At high temperatures it will form carbides, but is inert to non-carbide forming metals and is not wetted by many molten metals. Heating in air at 600°F enhances its adsorption properties. Because of RVC's large surface area, heating above 600°F in air will result in significant oxidation at rates which increase with increasing temperature.

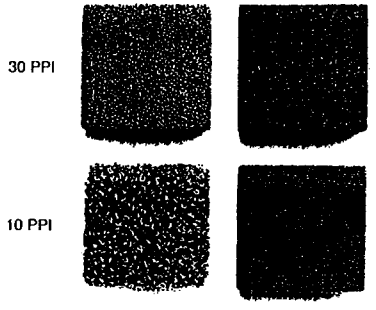

Several of the available pore size grades of RVC (PPI = Pores Per Linear Inch)

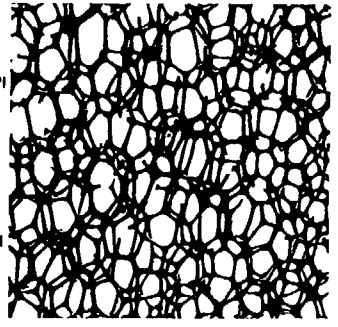

Enlarged view showing the open cell (reticulated) structure of RVC.

*Trademark

Aluminum Tube Sector Nr. 3
Five Disk Design

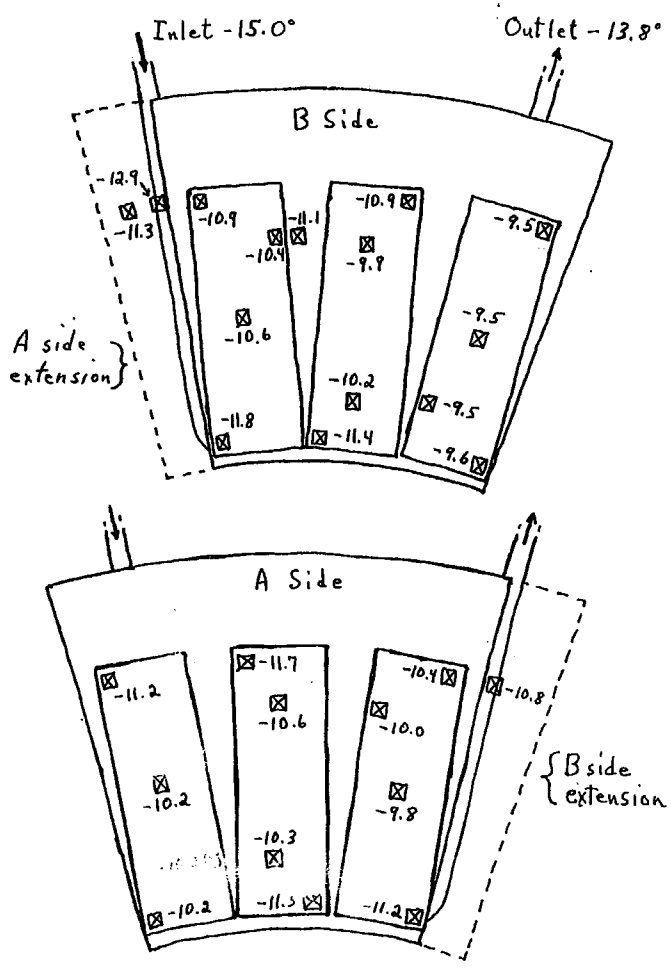

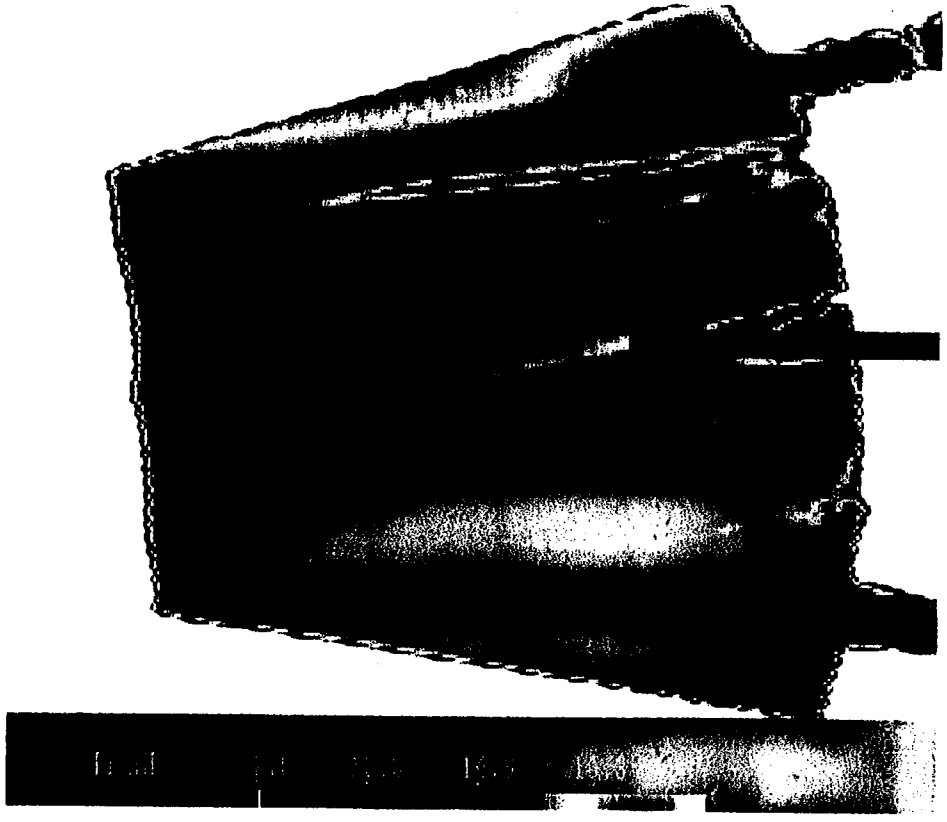

Coolant: 22% Methanol by volume, Flow 10 cc/s
ΔP = 196 mbar, Power 38.8 Watts, Ambient -9.2 °C
Adhesive for silicon: 85µ of CGL7018

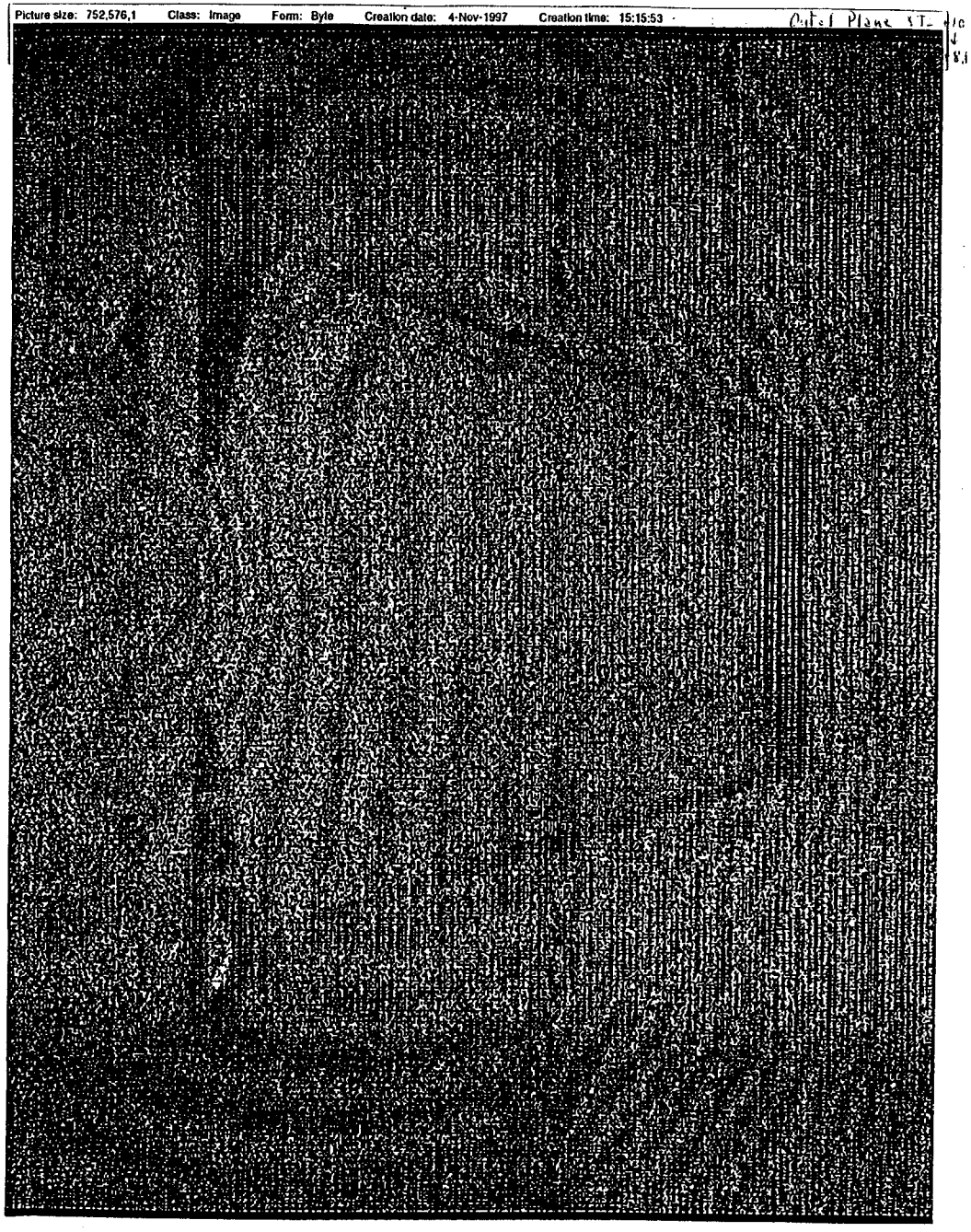

Prototype program 3: Carbon-carbon facings (0.5 mm thick), machined and sealed carbon-carbon or graphite coolant tube (3.2 mm id), may not need fill material.

Structural properties are assumed to be excellent as the sector is all carbon with no adhesives.

Prototype 2 radiation length of 1.24% can be reduce to less than 1.0% with reduced mass coolant tube.

Prototypes 1 and 2 had excellent thermal properties.

Main concern is sealing the carbon-carbon or graphite coolant tube. Coolant tube of prototype 2 has been sealed with Parylene and was found to have a Helium leak rate of approximately 10^{-6} cc/s after 24 hours of coolant exposure.

Module Attachment: investigating adhesives to provide thermal conductivity, electrical insulation, removability, and low stress

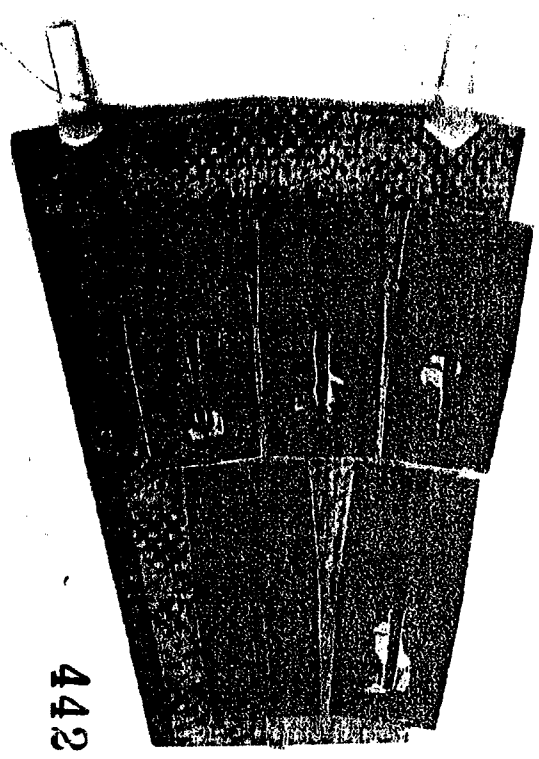

Silicon Adhesive Tests

Adhesive	Therm. Cond. (W/K*m)	Bulk Resist. (Ohm*cm)	Removable	Comments
AI Technology CGL7018	1.5	$9 * 10^8$	Yes	$X_0 \sim 15$ cm Curable paste
AI Technology CGR7018	1.6	$1 * 10^{12}$	Yes	$X_0 \sim 15$ cm Paste, Flows
Dow Corning 340	0.6	NA	Yes	$X_0 \sim 8$ cm Paste
Master Bond EP21AN	0.6	$2 * 10^{11}$	No	Room temp. cure
Thermagon 1KA08	1.6	$3 * 10^{12}$	No	Sheet adhesive
AI Technology CP7508-MP	0.5	$7 * 10^{13}$	Maybe	Mica sheet Brkdown >2.5kV
Cotronics Duralco 134	0.?	$2 * 10^8$	Yes	Paste
Norland NEA 123	NA	$> 10^{14}$	Yes	UV Cure For tacking

Radiation Tests have begun for items 1 and 3.

Infrastructure Session
May 8, 1998

W. Miller

Pixel Mechanics

- Topics-Pixel Detector Developments for LHC
  - Overview of ATLAS Pixel Detector
  - Disk Region
    - thermal design issues/choices
  - Primary detector structures-FEA Studies
    - outer frame structure
    - barrel and disk supports

ATLAS PIXEL DETECTOR

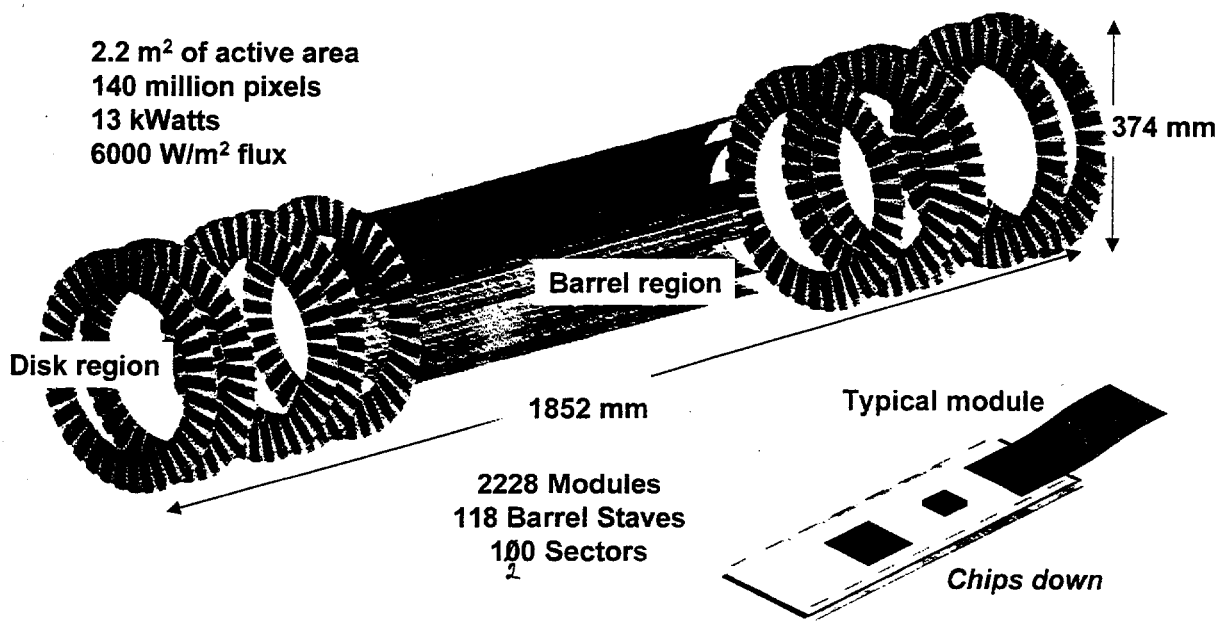

HYTEC INCORPORATED

Support Concept for ATLAS

General Arrangement

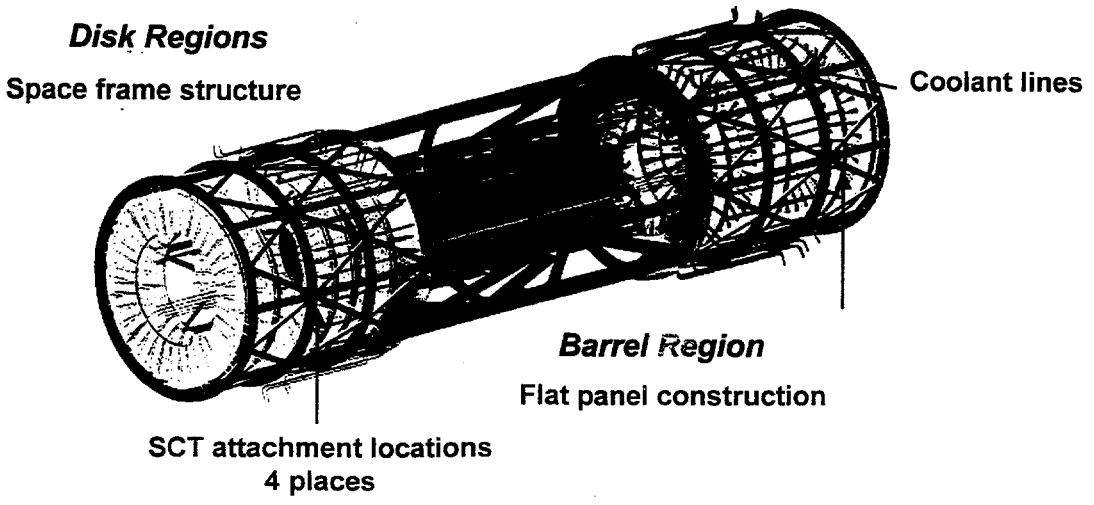

HYTEC INCORPORATED

Mechanical Design Issues

Issues

- Stability
  - Short and long term <10 μm's
  - Thermal strains from 40 °C change
  - Avoidance of flow induced vibrations--laminar flow
- Material limitations/Radiation length
  - High stiffness to weight ratio structures--stability problem
    - support mass 5 or times structural weight
  - Low Z Materials-- narrows options
- Cooling
  - Pixel array uniformly distributes heat
    - dictates use of coolant in tracking volume
  - Coolant thermal boundary effects
  - Coolant compatibility with module

Investigations

- Materials
  - Focused on ultra-stable composites
    - Radiation length second only to Beryllium
    - Extremely high stiffness to weight ratio
  - Introduced use of carbon-carbon composite for pixel module support (*widely accepted*)
    - Rad-hard
    - High thermal conductivity
    - Stiff and high strength
- Experimental studies
  - Sector thermal/stability tests
  - C_4F_{10}, and water-based testing
  - Thermal interface materials, rigid adhesives, greases, and gels
  - Sealing carbon-carbon channels

HYTEC

Pixel Detector Disk Region

Planar array
•5 Disks/Region
•12 Sectors/Disk
•Individually Supported
•Integral Cooling

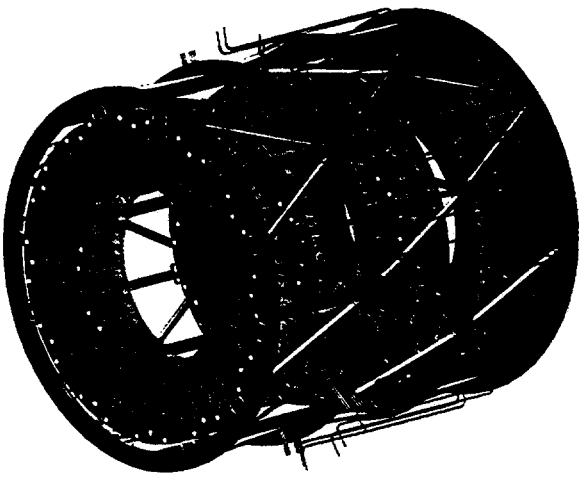

Stability
5 μm's φ
20 μm's Z
10 μm's R
Globally

Final Position
25 μm's φ
80 μm's Z
50 μm's R

General Concerns, both disk and barrel regions
•Heat Removal
•Detector Stability
•Local and Globally
•Precision Construction/Alignment

HYTEC

Pixel Disk Assembly

Disk with 12 Sectors

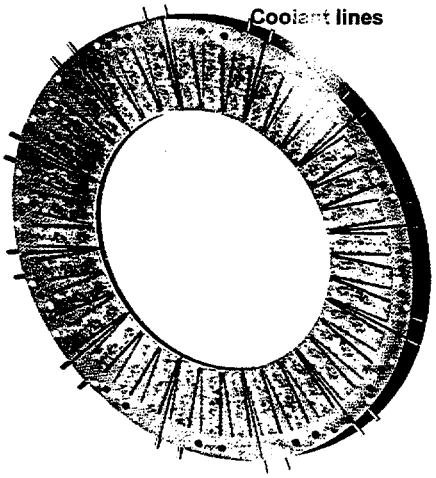

Sector support, cantilevered from outer edge

Enlarged view

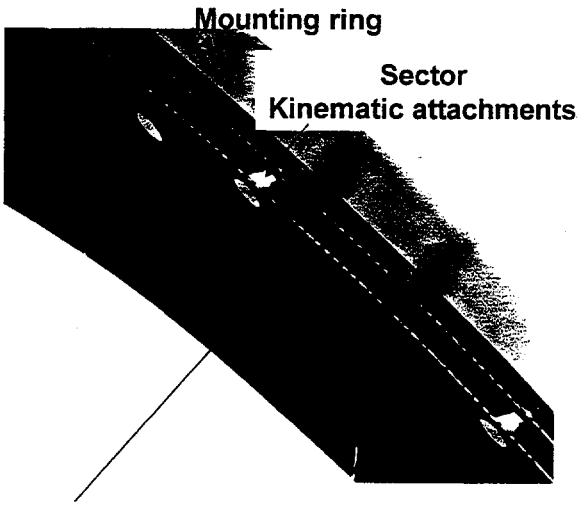

Carbon-Carbon thermostructure (fiber core omitted)

Temperature Gradient Issue- For 0.6 W/cm^2 (Cut-Away Of A Typical Sector)

- Potential ΔT's- °C
  - Adhesives 0.5 to 1.0
  - Module Carrier 6.0 to 0.5
  - Tube carrier 2.0 to 1.0
  - Grease Film 1.0 to 0.5
  - Cooling Tube 0.7 to 0.1
  - Coolant 6.0 to 2.0
- Probable Range 16 to 5
- Objective < 9.0
- *Actual ΔT's: Set by cooling fluid used, heat flux at tube surface, configuration, and materials chosen*

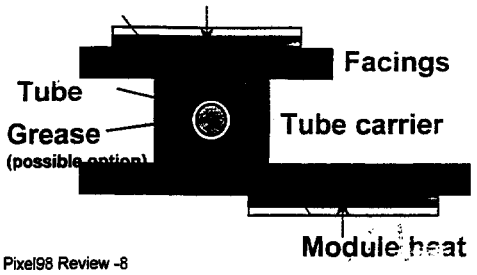

Sector with facing removed

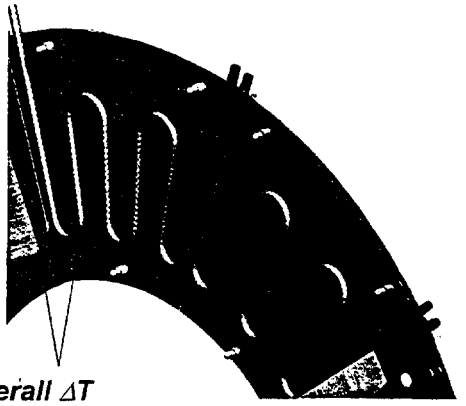

Overall ΔT module surface to coolant

Material Options -Limited To Low Z Materials

- **Metals**
  - Beryllium, best choice, 35 cm Radiation length
    - Disadvantage-High CTE
    - High cost
    - Can be brittle in thin sections
  - Aluminum, second choice, 9 cm Radiation length
    - Disadvantages, high CTE, poor radiation length
- **Composites**
  - Typical graphite fibers, XN50, P75, P120, etc.
    - Laminates have high stiffness to weight ratio, superior to metals
  - Low CTE
  - Demonstrated stability
  - Radiation resistant
  - Easy fabrication

Influence of different CTE's

(bi-metallic effect)

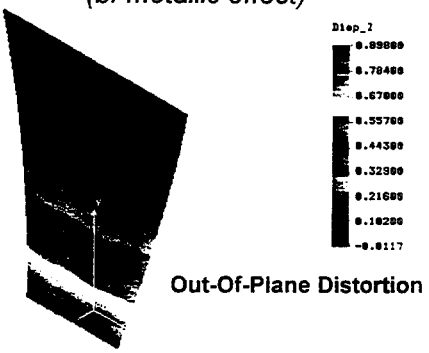

Out-Of-Plane Distortion

Single sector facing with 7 modules

- **C-C/Silicon, peak distortion 0.9 mm**
- ***Be/Silicon, peak distortion 1.92 mm***

Overcome this effect by a sandwich construction for the sector

Material Options-Composite Laminate Material Properties Polymeric Resin Systems Poor Thermostructure Choice

- Quasi-Isotropic laminate properties
  - For positive CTE close to silicon
    - Stiffness ~that of Al
    - Thermal conductivity very poor
      - K_{11}=8.9 W/m-K
      - K_{33}=0.7 W/m-K
  - High Modulus
    - Stiffness ~that of Steel
    - Thermal conductivity improves in-plane
      - K_{11}=200 W/m-K
      - K_{33}=1.2 W/m-K, Still Too Low
    - CTE becomes negative
      - CTE -1 ppm/ °C
- Benefit Of Carbon-Carbon Composite
  - Fiber (e.g. XN50)
    - $K_{11}=K_{22}$=185 W/m-K
    - K_{33}=25-40 W/m-K

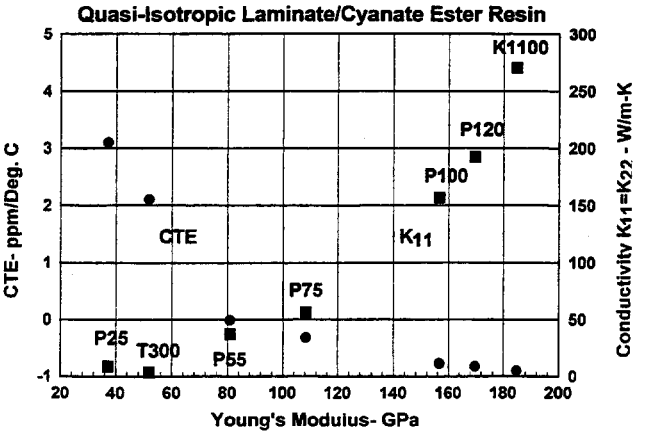

Sector Construction Concepts

- Selected criteria to achieve stability and thermal performance
  - Constructed from materials with low CTE's
  - Avoided mixing materials with significant differences in CTE's
  - Materials chosen on basis of high radiation length and high thermal conductivity
  - Sandwich structure with embedded coolant channel
- Sampling of prototype configurations
  - Carbon tube thermostructure
    - uses C-C carbon facings
    - carbonized structure
    - fiber core sandwich
  - Machined C-C channels, bonded sandwich with C-C facings
    - requires sealing C-C channel with resin or e.g., glassy carbon
  - Thin-wall C-C tube, bonded sandwich with C-C facings
    - well balanced CTE
    - high conductivity
    - options investigated for sealing are resin and glassy carbon

HYTEC INCORPORATED

Sector Cooling/Structure Developments

Bonded structures

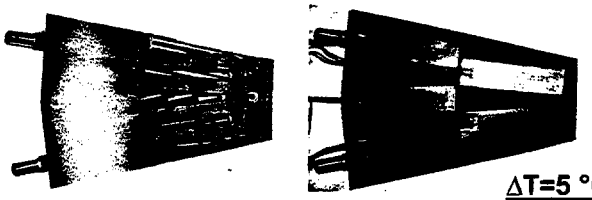

ΔT=5 °C

Machined graphite and carbon-carbon channels

ΔT=4 °C

C_C Tube/Bonded Interface

Carbon-carbon tube, 3.4 mm ID, 0.27 mm wall. Left side of figure shows the tube after densification; right side shows similar a tube after coating with glassy carbon.

Thermal Design Parameter: 0.1 W/mm @ tube
3.2 mm diameter tube

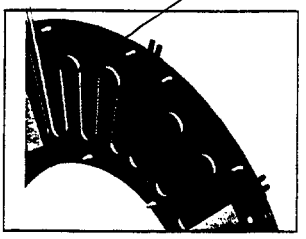

Carbonized structure

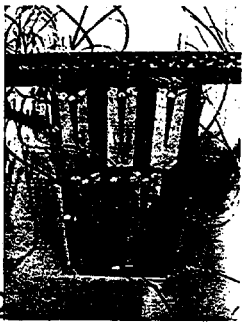

ΔT=9 °C

Early Prototype

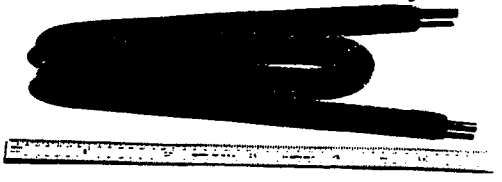

Carbon Tube/Fiber Carbonized Interface

HYTEC INCORPORATED

Detector Thermal Performance Experiments

Precise Thermal Measurements

Carbon-Carbon tube structure

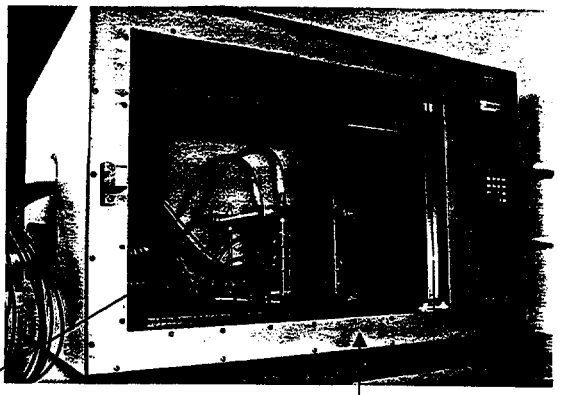

Chamber control +/- 0.1°C

Typical Sector

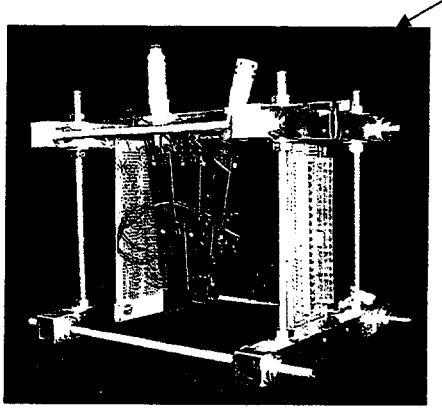

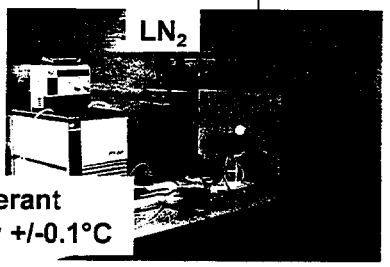

Refrigerant supply +/-0.1°C

Alcohol/water based coolant

HYTEC INCORPORATED

Stability Measurements/FEA Modeling

Experiments
(Oxford Univ.)

Desired Condition

10.6 °C ΔT

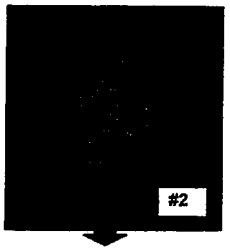

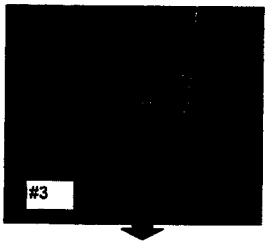

Low Core Shear Modulus

1.72 °C ΔT

Figure 6. Sector #2 fringe pattern for 10.6 °C temperature change (0.78 μm's local wafer bowing) and fringe pattern for Sector #3 (1.5 μm's bowing) for 1.72 °C temperature change.

Predictions

0.094 μm/°C

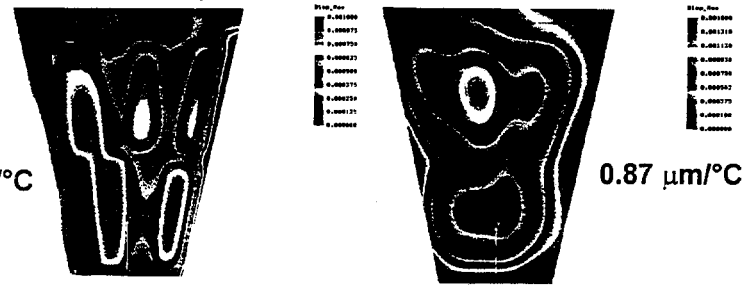

0.87 μm/°C

Figure 8. Finite element thermal strain solutions for Sector #2 and Sector #3, for temperature changes of 10.6 °C and 1.72 °C respectively. The predicted peak module deflections are 1 μm and 1.5 μm respectively. Approximate ESPI values of 0.78 μm's and 1.5 μm's respectively (Fig. 6)

HYTEC INCORPORATED

Detector Stability Measurements

TV Holography System under construction at HYTEC

Real-time thermal and vibration measurements

Example of Precision Bending and Twisting of a Cantilevered Wafer

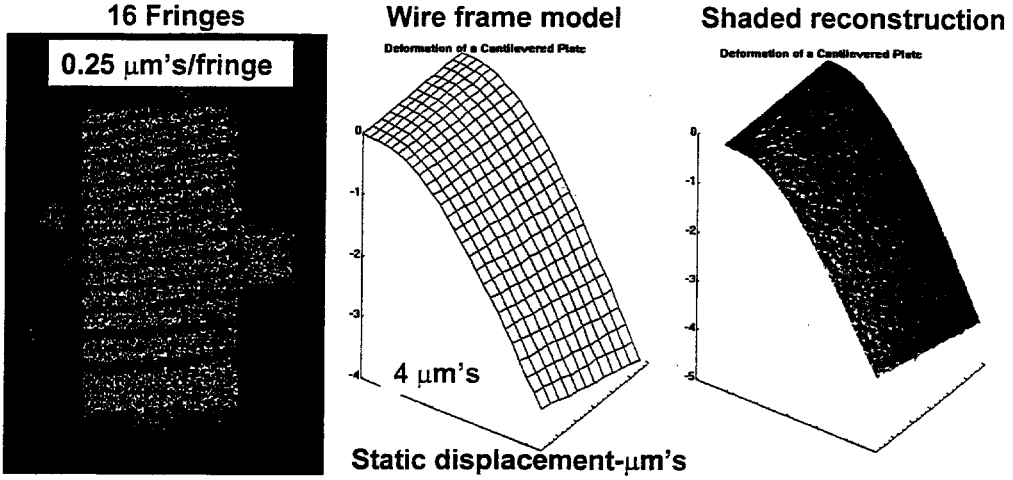

HYTEC INCORPORATED

Pixel Disk Sector

- Development progressing
  - desired thermal performance is attainable
  - investigations with C_4F_{10} evaporative fluid in progress and results are encouraging
  - stability testing far from complete
- Issues of mixing construction materials are not resolved, particularly different CTE's
  - cause thermal strains at times in excess of stability criteria
  - force solutions requiring compliant interface materials
- Most stable structure to date
  - achieved with carbonized thermal structure
    - little mismatch in CTE's
    - stiff sandwich construction

HYTEC

Pixel Disk/Support Dynamic Stiffness

Disk and Supporting Ring Structure

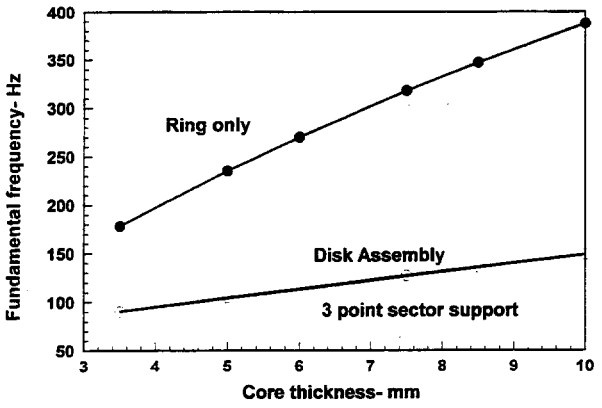

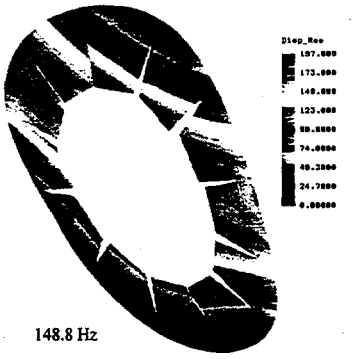

10 mm thick sandwich

Ring Parameters
R_o=210 mm R_i=180 mm

Sector
C-C Sandwich with fiber core

Pixel Disk Thermal Strains

- Support conditions
  - Three point support of composite ring
  - 12 sectors with three point rigid connection
- Materials
  - Sector, Carbon-Carbon, graphite fiber core sandwich
  - Ring, Carbon-Carbon facings, honeycomb core
- Temperature effects
  - Cool-down from room temperature, ΔT=40 °C

Out-of-plane illustration

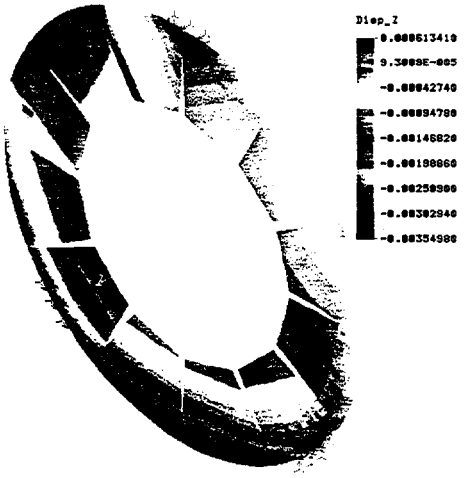

Peak sector displacement at support-3.5 μm's

Barrel Region Structures

Stable Ultra-Lightweight Composites

End Cones-composite sandwich- *0.31% R_L*

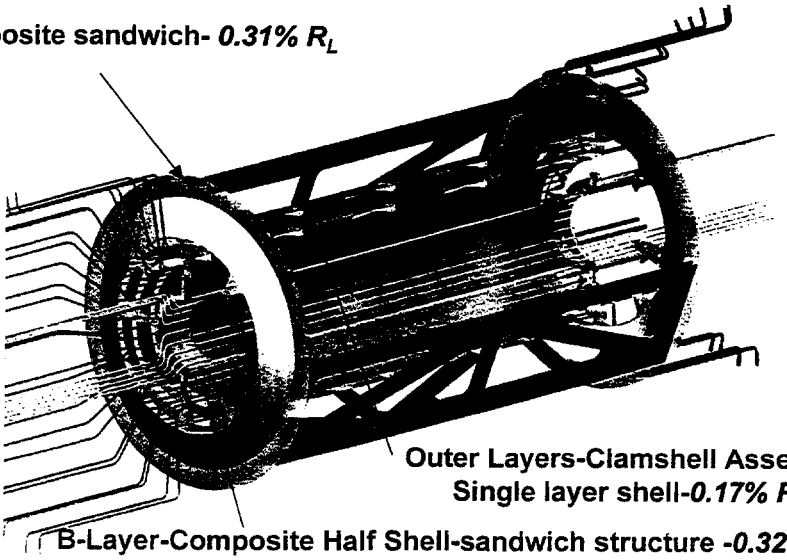

Outer Layers-Clamshell Assembly
Single layer shell-*0.17% R_L*

B-Layer-Composite Half Shell-sandwich structure *-0.32% R_L*
(Inserted into Inner Detector Assembly)

HYTEC INCORPORATED

Frame Studies Barrel Region

Individual FEA solutions

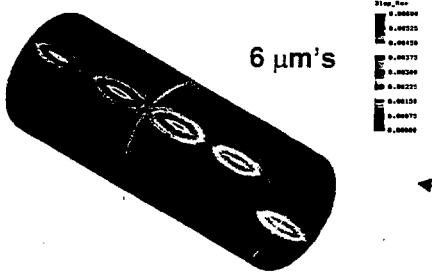

6 μm's

Outer Clamshell

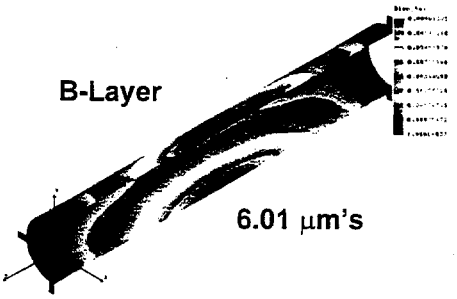

B-Layer

6.01 μm's

Combined Solution
Including effects of End Cones

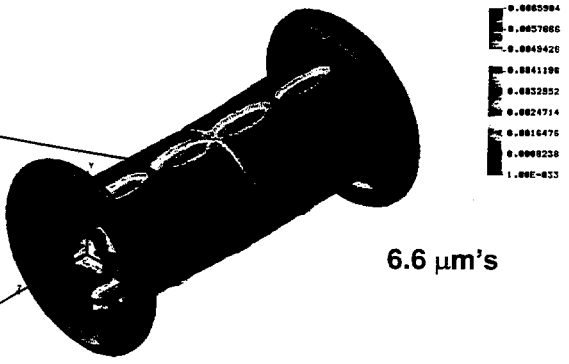

6.6 μm's

Mass of Stave/modules-8.7 kg's
Structure 1.98 kg's

45

HYTEC INCORPORATED

ATLAS Pixel Detector Weight Summary

Item	Number	Wt. Kg
Barrel staves	116	9.15
Barrel shells	3	1.43
Stave mounts	342	0.356
Disks	10	7.74
Interlinks-End Cones	2	0.387
SCT connection	2	0.47
Outer frame		2.66
Tubing (1/3 of mass)		4.8
Cables (1/3 of mass)		10.7
Total		37.693

HYTEC

PIXEL98 PIXEL WORK SHOP

Barrel Structure Dynamic Stiffness

Stable Ultra-Lightweight Composites

Typical laminate: XN50 fiber/cyanate ester resin

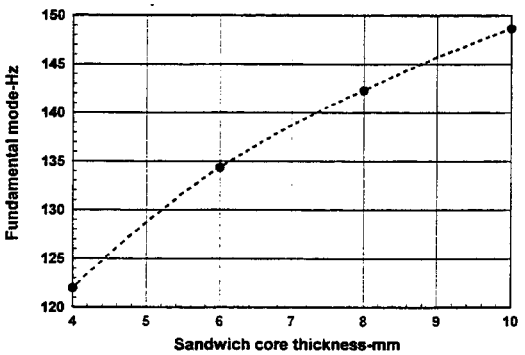

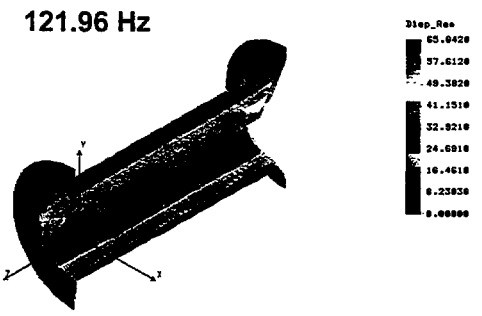

End cones with 4 mm core thickness

HYTEC

DESIGN STATUS OF THE CMS FORWARD PIXEL DETECTOR DATA TRANSMISSION: READOUT TO VME

Bruce A. Barnett

Department of Physics and Astronomy

Johns Hopkins University

3400 N. Charles. St.

Baltimore, Md. 21218 USA

Abstract

The CMS experiment at the CERN LHC includes a pixel system for tracking and vertexing charged particles. This system consists of two parts: the central and the forward detectors. This paper describes some features of the forward detectors related to data readout and power systems.

1 Overview

The initial design and research goals for the Compact Muon Solenoid (CMS) experiment for the Large Hadron Collider (LHC) at CERN have been specified in the CMS Technical Proposal [1]. The CMS pixel system includes a Central Pixel Detector and a Forward Pixel Detector, each having two pixel layers, as shown in Prof. Daniela Bortoletto's talk at this conference.

The four forward pixel wheels cover an annulus with inner and outer radii of 60 mm and 150 mm located on each side of the interaction region at Z =±325 and 465 mm. They extend the solid angle to $\eta = 2.44$. Each wheel consists of 24 wedge-shaped panels called blades. A "turbine blade" configuration is used in which each blade is rotated by 20° about an axis perpendicular to the p-p beamline. This layout takes advantage of the Lorentz ($\vec{E} \times \vec{B}$) effect and the large particle incident

angle to increase the charge sharing between neighboring pixels in the R and $R-\phi$ directions, respectively. Each blade is of trapezoidal shape with sensor arrays mounted on each side of a support structure. Square 150 μm pixel cells are used in both the forward and central pixel system.

A single readout chip (RO) is used in both the barrel and forward pixel system. It has a matrix of 52 columns and 53 rows of preamplifiers coupling through bump bonds to the individual pixel cells. A RO covers an area of 8mm x 10.45mm. Up to 10 RO chips connect to a single silicon pixel "plaquet". The detailed functions and drawings of the RO are described in talks at this conference by Kurt Gabathuler and Gary Grim.

2 Data transfer from RO to Portcard

The data from the RO is transfered to a "portcard", located near the outer edge of the blade. It transfers data to the outside world via an optical fiber system. The portcard is described in a talk at this conference by Bob Stone. The present design has 23 signals being transfered from the RO to the portcard: data(2), I2C bus (2), clock (2), trigger (2), reset (2), detector bias (1), guard ring current (1), monitors (3), counting token (4), and low voltage & grounds (4). The voltage levels are -2.5 V for the analogue and -5 V for the digital systems. The expected power is 40 microwatts/pixel for analogue and 10 microwatts/pixel for digital. These pixel currents translate into maximum currents from one supply of 5 amps analogue and 1 amp digital for the planned cabling scheme .

The communication between the RO and portcard will be done on multilayered Kapton cables. The limited space requires that there be a High Density Interconnect cable, or HDI, placed between the plaquets with connections to the RO using wire bonds. This cable runs in the $R-\phi$ direction, and will have three conducting layers, separated and protected by insulating layers:

1. The top conducting layer connects to the RO using wire bonds and carries the signals across

the HDI to vias connected to the third (lowest) layer. It also has conducting traces which carry the token counter signal from RO chip to RO chip expediting communication of the end of the readout of one RO and the beginning of readout from the next RO.

2. The middle layer carries the analogue and digital power input lines and their grounds. This layer will reduce cross talk between the regular signal lines. It also allows enough space for wider power and ground traces to reduce IR losses on the cable. The individual traces can be made of 0.5 oz copper and have 1.5 mm width. Vias from the top (first) to bottom (third) layer must pass through these traces.

3. The bottom layer carries the signals received through vias from the top layer out to the portcard. There is one trace on this layer for each of the signals, i.e. all of the information to and from the various RO chips are multiplexed onto this layer. For example, the 2 "data lines" or 2 "reset" lines on this layer feed to all the RO chips using the vias to the top layer. The trace widths and heights on this layer will typically be 150 and 25 microns, respectively, with 300 micron pitch.

A 90 degree bend is required in the cable to reach the port card. Two methods are now being considered to accomplish this.

1. The HDI cable could be made long enough to reach the port card where a simple fold would be made to change its direction from $R - \phi$ to radial.

2. The HDI could be wire bonded to a second, radial, 2-layer, cable, called a "pigtail".

The first method has the advantage of reduced cost and installation ease, but the disadvantages of more material and the danger of breaking traces by making the fold. Johns Hopkins University is communicating with Speedy Circuits, Huntington Beach, California regarding the technical and cost issues related to these cables.

Another issue to be determined is whether the sensor bias voltage is carried on this pigtail/HDI system or on a separate, dedicated wire. Because the pixel sensors will be adjacent to the cables it is simple to connect directly from the wire to the sensor bias lines. A coaxial wire of about 0.030 inch diameter manufactured by New England Electric Wire Corp could be used with a cost of less than a dollar per foot, not including connectors. Its radiation resistance needs to be checked. The advantage of a separate wire is that the potential 500 volts would not need to go through the portcard, and the voltage carrying capability of the HDI could be reduced. Also, procuring appropriate cable connectors is simplified. For example, the connector now used on the CDF HDI, manufactured by Berg Electrical, is rated only to 125 volts.

3 Optical Fiber Link

The CMS forward pixel project will use a fiber optics readout link to carry information between the central core of the CMS detector and the outside control systems. It will utilize the fiber optics specifications and equipment that is adopted by CMS for all of its other readout. CMS members of the RD23 research program are developing this system. A description of the data transmission from the pixels to the readout room serves to illustrate the general procedure. The optical link transmits analogue signals from the pixel transmitter hybrids to the readout room receiver hybrids. The dynamic range of the analogue signal will be 8 bits. The total path length is about 100 meters. Patch panels are included at each end to allow separability. Specifically, the forward pixel system will have patch panels about 30 cm from the portcards at the flexible interface of the support tube, another panel at the end of the service cylinder which is about 3.5 meters from the flexible interface, and then long fibers going to a patch panel near the VME crates.

A prototype analogue optical link has been developed and tested [2]. The link includes lasers, fibers and receiver PIN diodes representative of the devices intended to be used in the final system.

A version has been received by Johns Hopkins for testing and familiarization. Tests done by RD23 show that the system's pulse output shape has a bit of an overshoot, but that the pulse settles within 15 nsec to within 1% of the end value. This is within the required 25 nsec sampling period that is available at the LHC. The RD23 tests also show that the full system's relative distortion is well within the 2% linearity specified by the CMS requirements.

4 VME

The VME data collection system which the CMS Forward Pixel system uses will be as identical as possible to that of the rest of CMS. It may need some modifications to be completely compatible with the portcard system, but the intention is to keep modifications to a minimum.

5 Power Supplies

The characteristics of the power supplies for the CMS Forward Pixel system can be very similar to those used by the CDF SVX II system and by other CMS subsystems. The final vendor selection and power supply specifications will be made in conjunction with the other sections of the overall CMS collaboration.

We expect that a single cable will carry power for the chips and bias of a detector subunit. The number of sensor arrays and/or chips that will be assigned to a single supply is not yet determined. The decision on the routing will depend upon the current requirements for the final detector arrangement.

The bias power routing has been considered because we expect different sensor arrays will require different bias voltages. The biggest effect will result from the incident radiation which causes the required bias voltage to increase. The bias voltage is linearly dependent on the fluence after type

inversion occurs, which in turn depends upon the distance from the beam approximately as $R^{-1.6}$. Therefore, the radiation received, and the bias voltage required, for the inner sensor arrays at 6 cm can be quite different from that for the outer sensor arrays at 15 cm. Accordingly, we believe that sensor arrays at the same radial distance could share bias voltages, and that it would be unwise to assume that all sensor arrays on a specific blade can share bias voltages. For example, when a bias voltage of 400 volts is required at 6 cm a voltage as low as 90 volts might suffice at 15 cm. Care in avoiding ground loops will be required, however, in connecting sensor arrays from different blades to one another.

We expect that a system similar to the C.A.E.N. Model 527 would be suitable. This allows many channels with positive, negative or floating voltages to be controlled from a single point. CDF uses a system like this, but the sensor bias voltage for CDF is lower than CMS will need.

6 Acknowledgments

I wish to thank my many colleagues on CMS for their essential contributions to this research program. I also wish to thank the Department of Energy and the National Science Foundation for their support of the US CMS and LHC programs.

References

[1] The Compact Muon Solenoid, Technical Proposal, CERN/LHCC 98-6, April 20, 1998.

[2] Prototype analogue optical links for the CMS tracker readout system, V. Arbet-Engels, et. al., CMS Note 1997/075,

Progress on the CMS Forward Pixels-

Mechanical and Cooling

Lucien Cremaldi,[1*] Mike Booke,[1] Bruno Gobbi,[2] Bob Tilden,[2] Paul Rubinvov,[2]
Muzzafer Atac,[3] Jay Hoffman[3]

[1] University of Mississippi, [2] Northwestern University, [3] Fermilab
* Presented at PIXEL98 – International Pixel Detector Workshop, Fermilab
May7-9 1998.

It is widely recognized that inner pixel tracking detectors can play an important role in the LHC's quest for new physics discoveries. The CMS pixel detector provides critical b-jet tagging and pattern recognition capabilities for the tracker near the busy collider interaction region. Over the past year this system has undergone significant design changes and testing of components. A brief description of recent progress in the design of the CMS forward pixel wheels is presented. More details are contained in the CMS Tracking Detector TDR [1].

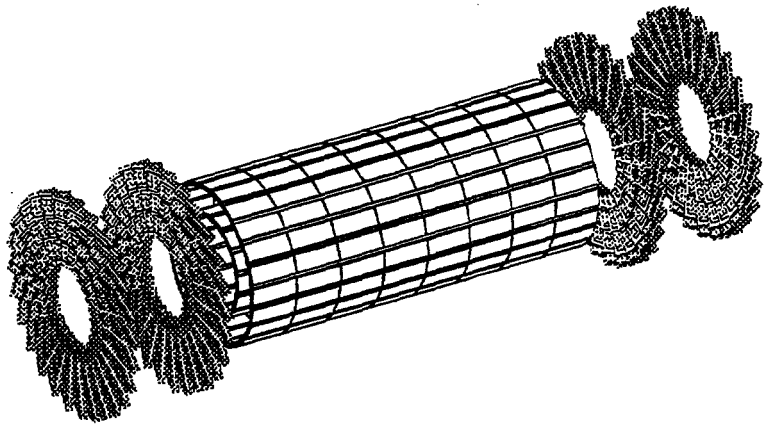

Figure 1: CMS Forward and Barrel Pixel Detectors.

Mechanical Design

The CMS forward pixel system consists of a two layer barrel and a two layer forward detector covering a range of pseudorapidity out to $|\eta| = 2.5$. The two forward pixel detectors are positioned at z=32.5 cm and z=46.5cm respectively. The radii of the wheels range from r = 6. cm to r=15. cm. The forward system is arranged in a turbine blade geometry, shown in Figures 1 and 2.

The following criteria are viewed to be of major importance in the design of the pixel system:

(1) The material budget must be minimized to a few percent of a radiation length to reduce electromagnetic showering into downstream detectors.
(2) The detector should be stable in position to an accuracy of less than±.01mm over a period of a few days, allowing slow alignment drifts to be tracked though the run.
(3) The pixel sensors must be kept at approximately T=-5degC during operation to prevent reverse annealing and the electronics must be kept uniform and stable to within ±1degC.

(4) Distortions due to changes in the operating temperature must by held to within ±.01mm over a few day period.
(5) The pixel detector must be fabricated in 2 halves to be inserted around the beam pipe after a beam pipe bakeout period.

Each of the four forward detector disks consists of 24 wedge-shaped blades (12 per half-wheel) which hold the pixel sensors and electronics. A cooling channel services four to six blades in series. Each blade assembly is rotated at 20 degrees to enhance charge sharing, forming the turbine-blade geometry.

Points of interest shown in Figure 2 are :
(1) That the cooling tubes form a structural part of the half-wheel assembly, thus reducing total material.
(2) The tubes are attached to an inner and outer carbon-fiber ring to complete this structure.
(3) Internal alignment of the system with tracks is made easier by a small blade-to-blade overlap as well as a front-to-back sensor overlap.

The detectors must be installed from points along the beam at z= 3m after a bakeout of the beam pipe. To aid in this installation the half disks are installed in a space cylinder, shown in Figure 3, which is attached to a permanent service cylinder. Between space and service cylinders all electrical, optical, and service connections are made. These low mass carbon fiber space and service cylinders are moved into place on a system of rails which are attached to the inner layer of the silicon strip detector (not shown). The service cylinder will also provide a buffer area for commissioning the pixels during early installation procedures.

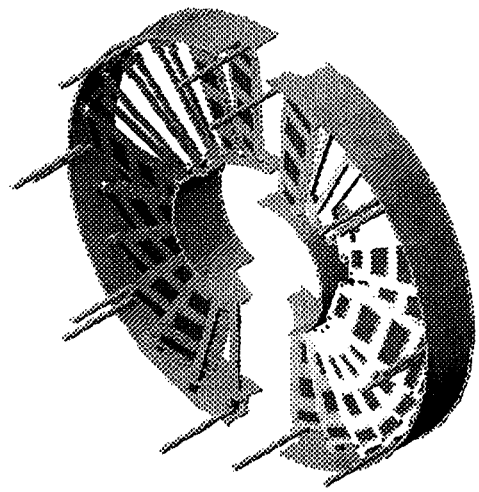

Figure 2: View of detector blades mounted in half-wheel configuration with cooling pipes.

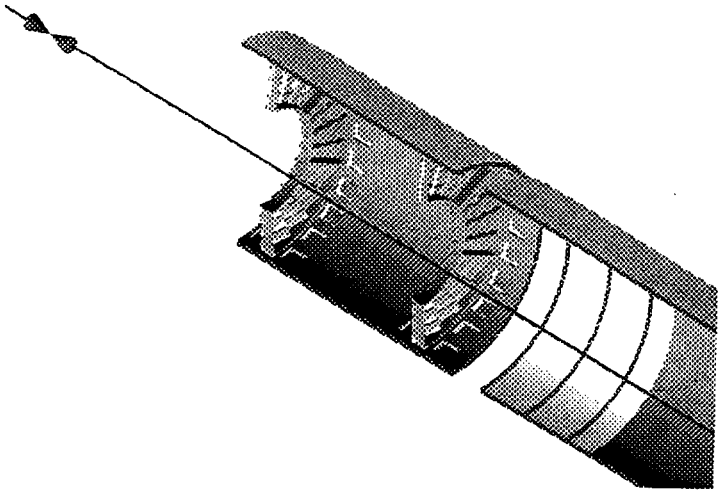

Figure 3: Forward pixel half-wheels are shown mounted onto its space cylinder. A portion of the following service cylinder is also shown.

Each blade is constructed from two low mass c-c carbon panels [2] mounted to an Al (0.2mm wall) cooling tube which runs directly under and at the edge of the electronic readout/sensor arrays. The c-c panels are aligned with respect to the cooling pipe by an alignment frame directly attached to the cooling pipe. An exploded view of the blade assembly is shown in Figure 4.

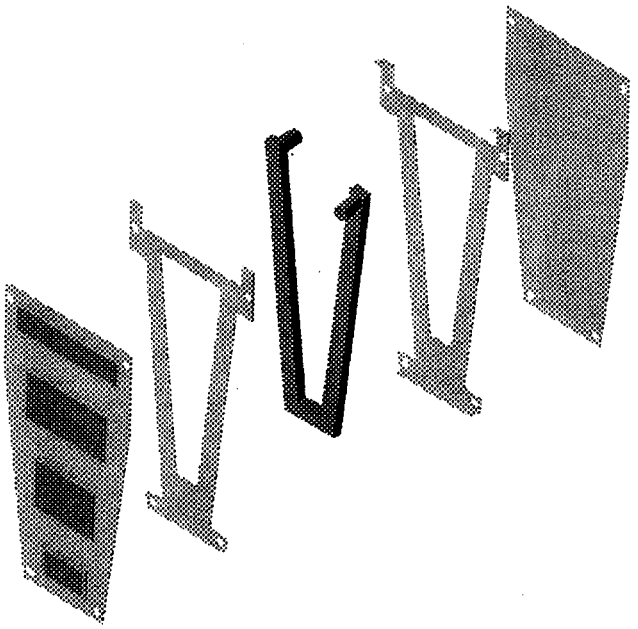

Figure 4: Exploded view of forward pixel blade, with cooling pipe and alignment frame.

Pressure Drop Measurements

Of special concern is the pressure drop in the U-tube sections of the detector blade assemblies. For safety reasons we want to maintain a pressure drop of <500mbar across the interior detector. A series of pressure drop measurements have been completed with water flowing at 20deg C. In these tests an open air and digital manometer apparatus was used to measure the pressure drop in a series of U-tubes similar in design and cross section to those proposed for the blade.

For calibration purposes straight tubes of various cross sections were tested and pressure drops compared to the Darcy equation $\Delta P = f\,(L/D)\,\rho v^2/2$ where P(pa) is pressure. L(m) is tube length, D(m) is tube diameter, $\rho(g/cm^3)$ is the density, and v(m/s) is mean fluid velocity. The friction factor is f=64/Re for laminar flow (Re < 2600) and can be parameterized in the turbulent zone. In Figure 5 we show the pressure measurements for a number of straight tube cross sections of length L=30in. The onset of turbulent flow is at approximately (8-10)cc/s for this liquid.

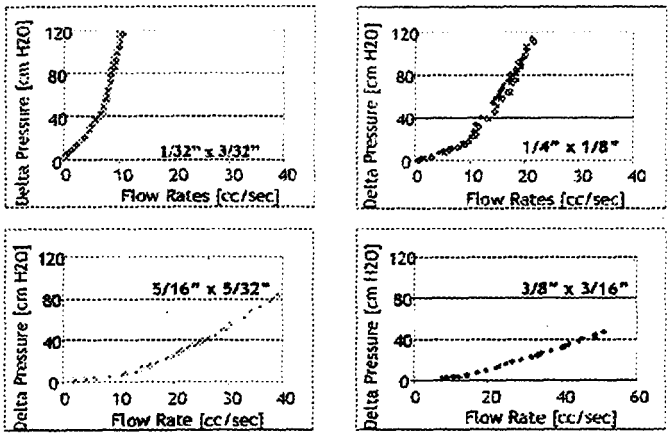

Figure 5: Pressure Measurements of straight tube section s of indicated cross sections.

The present design calls for a series connections of 4 to 6 U-tubes. Additional friction factors accounting for the pipe bends have been studied. These results are presented in Figure 6. A coolant like HFE-7100 at –15deg C has a viscosity similar to that of water at (20deg C) and 60% higher density. Thus the 6-U-tube result shown below and measured with water implies that the pressure drop across a 6-U tube configuration will be somewhat less than 200 mbar for flows of (5-10)cc/s.

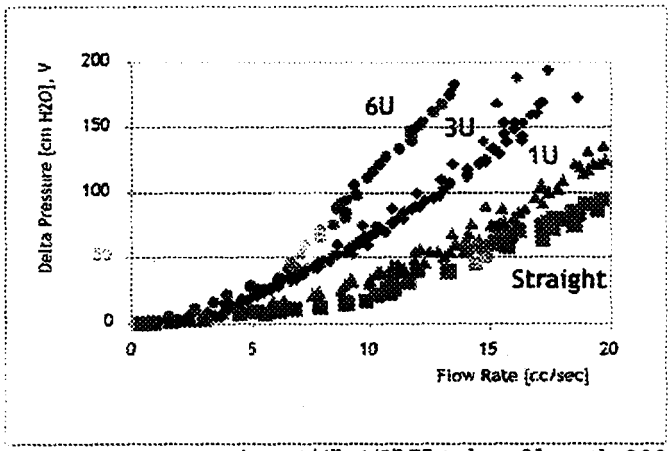

Figure 6: Pressure drop measurements in a 1/4"x1/8" U-tube of length 200mm for the indicated configurations.

Pixel Detector Cooling

Current estimates for the forward detector heat load including electronics are based on 66μW per channel for readout electronics and sensor. With 2756 pixels per chip and 45 chips per blade, each blade will heat to 8.2W. Adding an additional 50% for laser drivers, control chips, cables, and heating from IR losses in the service tubes, we estimate 1.2 kW of total power for the 4 disks.

The power load on the cooling tubes is expected to be 40mW/cm at the cooling pipe. We project that the sensor temperature must be maintained at T~ -5deg C to minimize reverse annealing biases. To cope with expected temperature differences due to thermal resistance and limited heat transfer a coolant inlet temperature of T~ -15deg C is required. Since the coolant must be supplied through long tubes with the smallest possible cross section, a liquid having a low viscosity at this temperature is most suitable. For safety reasons it is desirable that the coolant be electrically isolating, non-flammable, and non-toxic. A non-flammable and medium radiation length fluid from 3M, hydroflouroether HFE-7100 from 3M [3], is now under consideration.

HFE-7100 ($C_4F_9OCH_{10}$) is a clear, colorless, and low-odor fluid intended to replace ozone-depleting materials. It's chemical and thermal stability (Boiling Pt.= 61degC, Freezing Pt.=-153deg C) and non-flammability make it extremely useful for heat transfer applications. Materials compatibility tests performed by 3M have shown it to be safe to use with Al, low carbon steel, and titanium tubing, and many plastics and rubbers.

HFE-7100 has relatively poor thermal conductivity and near turbulent flow conditions may be necessary to effect proper cooling. In Table 1 we give material properties, flow, and pressure drop parameters for a system capable of removing 8W of power from a pixel blade. Ethanol(35%)/Water coolant is included for comparisom. Development of potentially lower mass evaporative fluorocarbon cooling techniques is also being pursued with fluids such as C_4F_{10} [4].

ρ(kg/m^3)	Cp(J/KgK)	K(W/mK)	μ(mPas)	Xo(cm)	dm/dt(g/s)	Re	ΔP(mbar)
(a) 1682	1096	.077	1.15	23.	8.8	2693	15
(b) 963	4045	~.55	30	34.	2.4	28	98

Table 1: Properties of (a) HFE-7100 coolant (b) Ethanol(35%)/Water at T=-20degC. The pressure drop and flow rate are also given for removing 8W of power through a L=220mm and σ =10mm^2 U-tube.

Selection of low mass and radiation resistant materials forming a low resistance heat path to the cooling channel is of utmost concern. The thermal resistance/temperature drops along the cooling path must be carefully studied as not to impede the heat flow. We mentioned previously that the pixel electronics will be bonded to a .3mm c-c panel[1]. This material has an in-plane thermal conductivity K_{ab}= 200 W/m-K and through-plane conductivity K_c= 30 W/m-K. These c-c panels have been shown to work well in conducting heat to the cooling tubes. A small temperature drop of < 3deg C is observed from center to edge of the electronics mounted on the c-c panel with a few tenths deg C drop through the c-c panel. The panel is greased to a .3mm thick c-fiber alignment frame, which is glued to the cooling tube. Measurements and calculations confirm about a 0.5deg C temperature drop through this structure from panel-to-pipe, although care must be taken at this junction. There is an additional 3 to 4deg C drop from pipe-to-bulk fluid (depending on cooling fluid), giving a total ΔT ~ 8deg C. A fluid circulating at bulk temperature T(bulk)=-15deg C is projected to keep

the pixel electronics at approximately T(electronics)~ –7deg C. The projected temperature drops based on ANSYS simulations and conductivity measurements are shown in Figure 7.

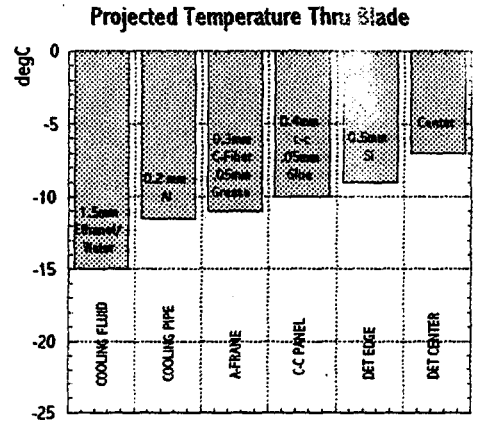

Figure 7: Projected temperature profile through a blade.

Cooling Tests

Thermal tests have been performed on prototype blades fabricated with c-c panels. Ethanol(35%) /water was used as coolant. The top and bottom panels are greased to a σ =7.6 mm^2 by L= 180mm cooling tube running along the edge. Coolant is supplied at -15degC. An 8W heat load is applied by an array of thermofoil heaters [5] carefully placed to mimic the pixel electronics. RTDs[6] measured the temperature profile on the simulated electronic packages. A schematic of this system is shown in Figure 8.

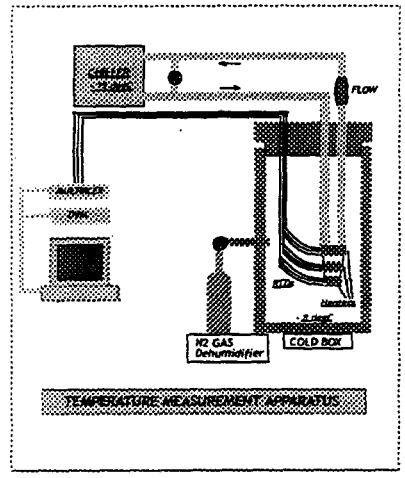

Figure 8: Schematic of apparatus used in the cooling tests.

The heat transfer mechanism is dominated by conduction to the cooling pipe, with small radiative and air-convective components. To minimize these effects the prototype wedges are tested in a dry-nitrogen filled cold-box nominally held at the surface temperature of the electronics (-7degC), also Figure 8. The inlet-to-outlet bulk fluid temperature increase for a single blade is measured to be ΔT(blade)=~1.5degC, collant flowing at 4.5cc/s. The mean electronics temperature on the blade is -5.8degC in this test. A typical temperature profile of the temperatures at the sensors is displayed in Figure 9.

Substrate thickness, glues, and greases are being optimized for thermal effectiveness, radiation survivability, and material budget. But already these tests have shown that adequate pixel cooling is feasible with this design.

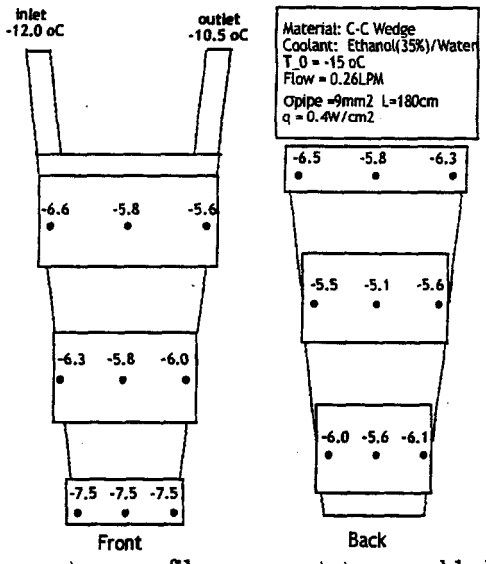

Figure 9: Measured temperature profile on a prototype c-c blade.

Refrigeration System

A system of refrigerators and circulating elements is being designed to provide cooling and dissipate the heat loads generated in the pixel, silicon, and MSGC tracker volumes for the CMS detector. Cooling supply lines for the forward pixels will enter near the beam pipe at a z = ±3m after long run from a central refrigerator complex. These supply lines must be compact and insulated insuring a small temperature drop from refrigerator to pixel enclosure. The bulk fluid temperature should be about T_b=-15degC. Supply and cooling pipe diameters are chosen to keep pressures below 1 bar at all points in the system. The circulation system should be designed with appropriate sterilization, particulate filters, de-ionizers, inspection stations, and sample ports as seen necessary. Evaporation tanks, air separators, spill tanks, etc. should be designed into the system. Of special concern will be the capability of this system to abort power to the pixel electronics or be fail-safe in case of emergency. Preliminary measurements have shown that the system has cooling latency sufficient to keep the sensors below room temperature for several minutes after coolant flow has stopped, giving ample time to abort power. We have calculated the total pressure drop in a conceptual refrigeration system flowing HFE-7100 to be approximately 650mbar across the inner pixel detector U-tubes + pixel detector service tube + 15m inlet and outlet service lines. We are presently working on the engineering design of a full test facility to verify these results.

Radiation Damage Measurements

We have begun to investigate a small sample of glues and epoxies for radiation damage properties. Our purpose is to find a low to medium viscosity, room temperature curing epoxy which we can use to bind silicon chips to the c-c panels. We believe a 5 mm thick layer is more than adequate for bonding, exhibiting little thermal resistance. The bond should retain over 75% of its strength after irradiation with Co[60] gammas. In these investigations samples of silicon are bonded to c-c material and standard shear tests are performed before and after irradiation of 10^7rad. Presently we are testing EPON [7] epoxies with TETA hardeners.

We show the result of some of our first tests (Figure 10), in which multiple samples of carbon/Si/carbon assemblies are bonded with epoxy mixes of different viscosity. The samples are pull-tested before and after irradiation, measuring the breaking shear force in pounds per sq. in. (psi). Our first tests have shown that upon radiation the samples have retained practically full strength and would be acceptable. Further testing under gamma, charged particle, and n radiation is envisioned.

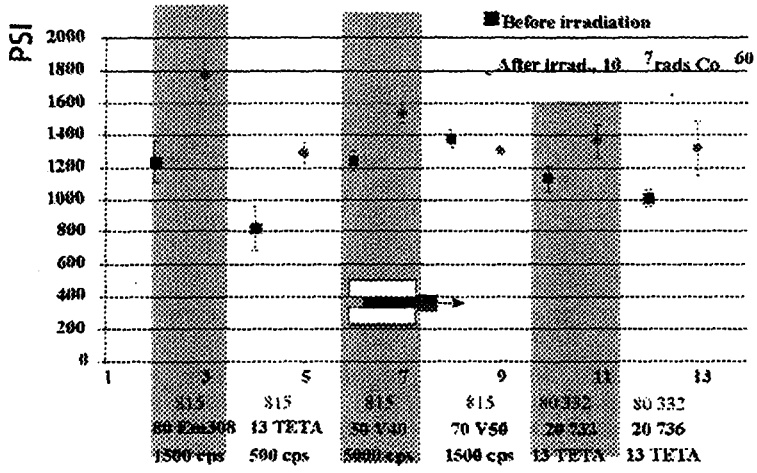

Figure 10: Shear test results for carbon/Si bonds with EPON epoxies.

Conclusion

Significant progress has been made in the mechanical design and testing of components for the CMS barrel and forward pixel detectors. Future work is focused on the optimization and final selection of materials, as well as complete engineering designs.

REFERENCES

[1] CMS Tracking Detector TDR, the CMS Collaboration.
[2] B.F.Goodrich Aerospace, Santa Fe Springs, CA.
[3] 3M Performance Chemicals, Minneapolis, MN.
[4] see talk by Greg Hallewell at this conference.
[5] MINCO Products Inc., Minneapolis MN.
[6] Omega Engineering Inc., Stamford CT.
[7] EPON, a registered trademark of the Shell Oil Company.

Experience with the SLD Vertex Detector

or

300 Million Pixels Can't Be Wrong

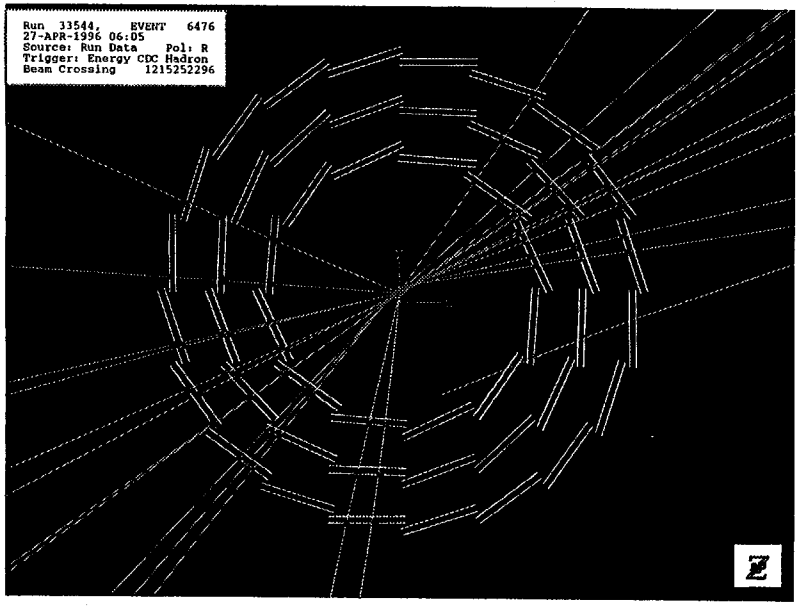

Glen Crawford, SLAC

Pixel 98 / Fermilab

- Detector Cooling/Mounting/Alignment
- Data Flow

NUCLEAR INSTRUMENTS & METHODS IN PHYSICS RESEARCH
Section A

Nuclear Instruments and Methods in Physics Research A 400 (1997) 287–343

Design and performance of the SLD vertex detector: a 307 Mpixel tracking system[1]

K. Abe[a], A. Arodzero[b], C. Baltay[c], J.E. Brau[b], M. Breidenbach[d], P.N. Burrows[e], A.S. Chou[d], G. Crawford[d], C.J.S. Damerell[f,*], P.J. Dervan[g], D.N. Dong[c], W. Emmet[c], R.L. English[f], E. Etzion[g], , M. Foss[d], R. Frey[b], G. Haller[d], K. Hasuko[a], S.S. Hertzbach[h], J. Hoeflich[d], M.E. Huffer[d], D.J. Jackson[f], J.A. Jaros[d], J. Kelsey[c], I. Lee[c], V. Lia[c], A.L. Lintern[f], M.X. Liu[c], S.L. Manly[c], H. Masuda[d], A.K. McKemey[g], T.B. Moore[c], A. Nichols[f], T. Nagamine[a], N. Oishi[i], L.S. Osborne[c], J.J. Russell[d], D. Ross[e], V.V. Serbo[j], N.B. Sinev[b], J. Sinnott[c], K. Skarpaas VIII[d], M.B. Smy[k], J.A. Snyder[c], M.G. Strauss[h], Su Dong[d], F. Suekane[a], F.E. Taylor[e], A.I. Trandafir[h], T. Usher[d], R. Verdier[c], S.J. Watts[g], E.R. Weiss[l], J. Yashima[a], H. Yuta[a], G. Zapalac[l]

ELSEVIER

VXD3 Milestones

- **Mar 94** VXD3 project approval.
- **Oct 94** Detailed design report completed.
- **Feb 95** First prototype CCDs arrive at SLAC.
- **Apr 95** CCD production phase begins.
- **Sep 95** First production devices shipped.
- **Dec 95** Delivery of production CCDs complete.

  VXD3 assembly and survey completed.

  VXD3 arrives at SLAC.

  Electronics and cryostat assembly in clean room.
- **Jan 96** Completed assembly mounted in SLD.
- **Feb/Mar 96** Extensive testing/debugging.
- **Apr 96** First VXD3 data logged.
- **Jul 96** End of commissioning run.
- **Aug 96** Detailed detector alignment begins.
- **Jun 97** Initial detector alignment complete.
- **Jul 97** Long datataking run begins...

Detector Cooling

Requirements

- **Maintain detector at operating T** (185 ± 1 K)
  Operating T set by minimizing in rad. damage
  Range set by need for alignment stability
- **Small heat load from detector** ($\sim$ 20W)
  $\rightarrow$ *no need for conductive cooling of detector substrate*
  Small heat loss from cryostat ($\sim$ 20W)
- **Low humidity to avoid condensation**

Solution: Boil-off LN_2

- Fed from dewar at 1gm/sec to 2-stage boiler
  Exit @ 135K to long ($\sim$ 15m) stainless vacuum lines
  $\rightarrow$ *most of heat loss is in cold gas transfer ($\sim$ 200W)*
- N_2 gas pressurizes small cylinder btwn beam-pipe + gas-shell:
  $\rightarrow$ *slow, radial gas flow over vertex detector*
- Outflow via similar (larger radius) vacuum lines, vent
  $\rightarrow$ *measure flow rate, pressure, moisture*

Cooling Details

Operating Parameters

- **Total temp. gradient in cryostat:** ~ 30 C
- **Total temp. gradient in detector:** ~ 15 C
- **Pressure in cryostat:** ~ 1.7 mbar
- **Moisture in cryostat:** ~ 2 ppm H_2O
- N_2 **flow rate:** ~ 60 liters/min

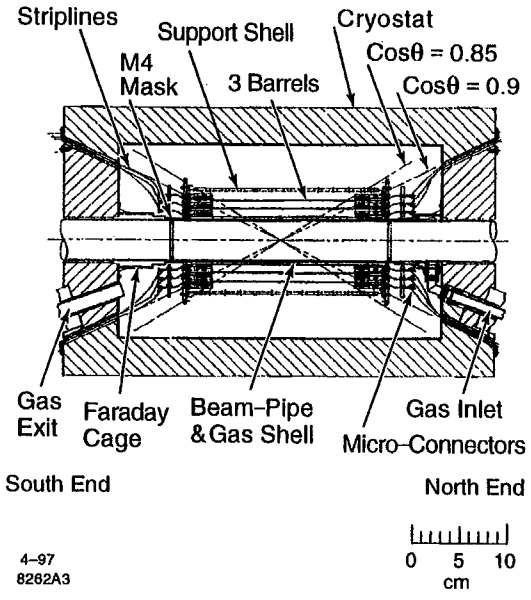

4/1

Cryostat

Basically a zero-mass, zero-strength foam cooler

- **Polyisocyanurate foam with filler gas**
  Denser foam in endcaps; lighter in barrel
  Also in last $\sim$ 1m of inlet gas pipe (in tracking solid angle)
  $\rightarrow$*inlet strengthened with carbon fiber sleeve*

- **Built in 6 sections (2 half-cylinders, 4 half-endplates)**
  Sealed with low-temp. silicone adhesive [NuSil]
  Penetrations for beam-pipe, stripline connectors
  Heater wire at joints to prevent condensation

- **Largest heat leak: beam-pipe**
  More heater wire to maintain beam-pipe $T > 15$ C

- Also a Faraday cage to shield detector from RF, elect. pickup

Mechanical Design Overview

Design goals: low mass, stable, repeatable assembly

- **CCDs mounted on Be substrates**
  - Substrates attached to annuli w/spring-retention blocks
  - Annuli attached to cylindrical Be support structure

  [Be chosen over C Fiber, Al for better isotropy, CTE match]

- **Assembly and survey done layer-by-layer**
  - Several special jigs to ensure repeatability
  - All components held + overconstrained by dowel pins
  - All adjacent components match drilled and reamed
  - All mating surfaces lapped flat and specially cleaned
  - Final installation in half-shells around beam-pipe

- **Outer Be support shell a "mesh" for survey, gas flow**

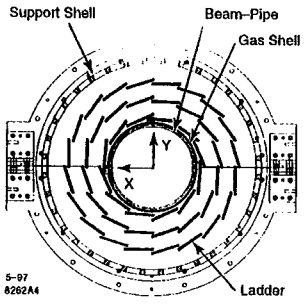

4?2

5-95
7934A1

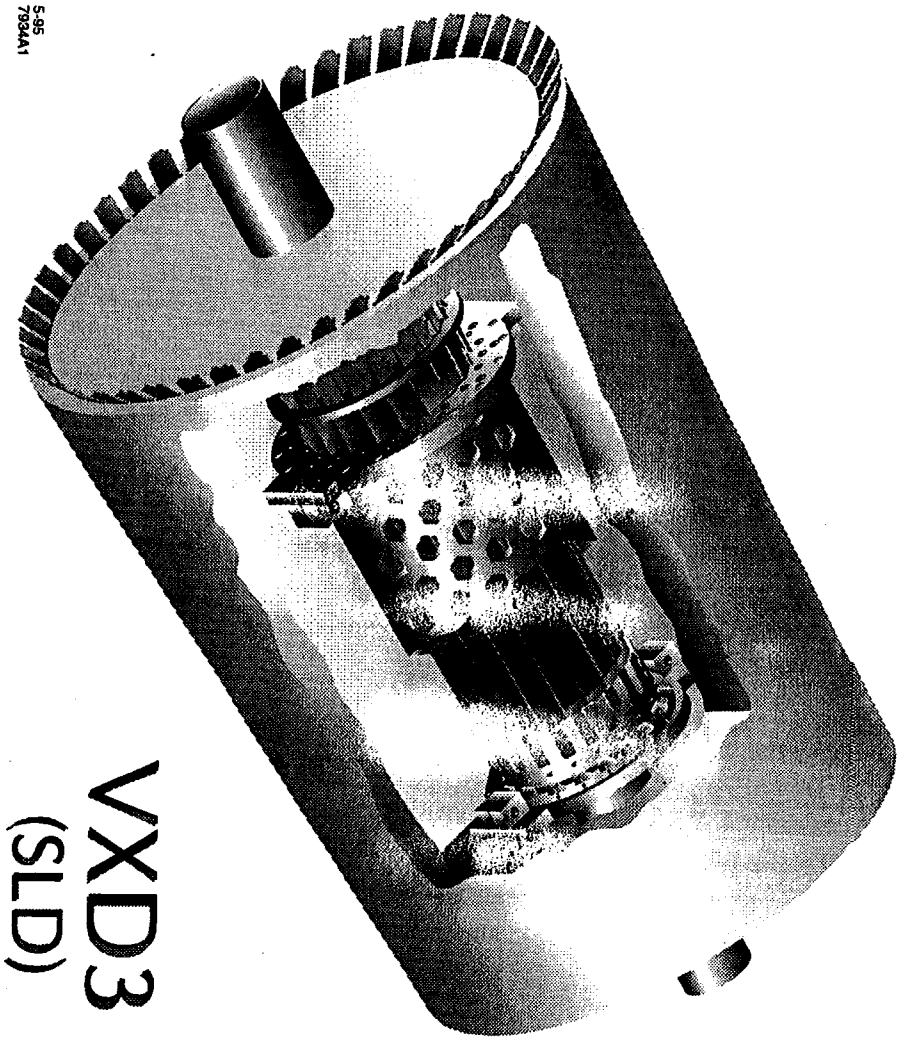

VXD3
(SLD)

CCD Motherboards

Most challenging component to design (most constrained)

- **Solution: Thin Be beam (380 μm)** [BeO too fragile]
  + 2 Copper/Kapton flex circuits
    (13 μm Kapton, 18 μm Cu + coverlayer)
  + "pigtails" to μconnectors

- Bonded with acrylic adhesive at $T \sim 180$C
  Tested for de-lamination

- CCDs attached with adhesive pads and wire-bonded

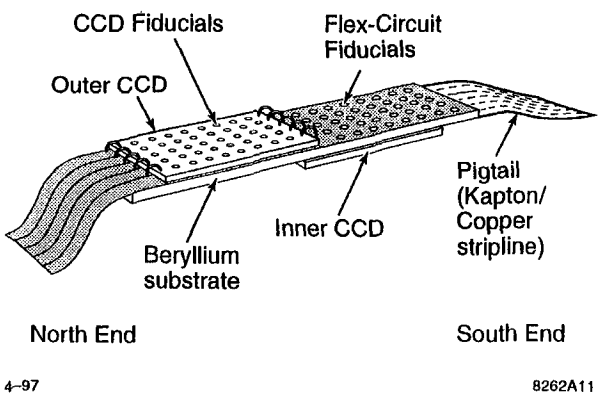

4 of 3

The CCD Sandwich

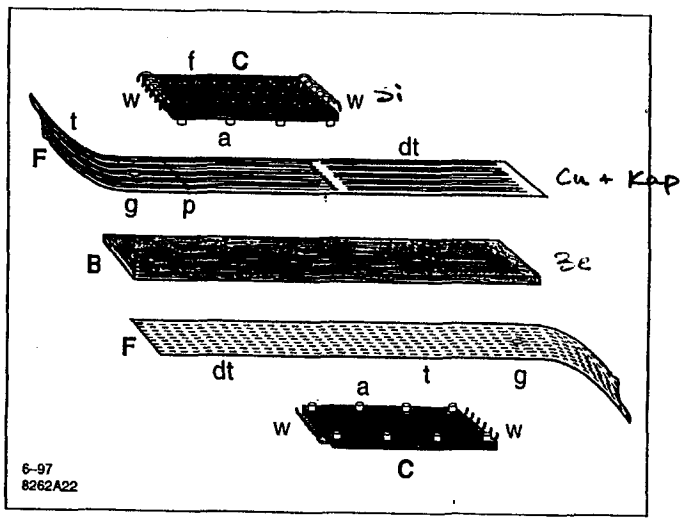

- Put 2 CCDs on a thin (15 mil) Be beam .11% RL (Be
  + .16% (CCD
- + Kapton flex circuits + .05%
- + Cu traces + Au bond pads + wire bonds + .09%
- + Adhesives (incl)

Σ = 0.40% RL

$\Rightarrow$ of 1.15% RL VXD2

The CCD Sandwich

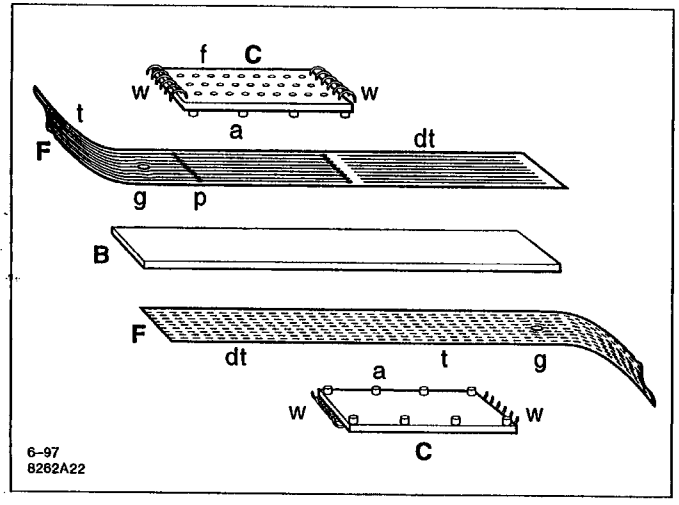

- Put 2 CCDs on a thin (15 mil) Be beam
- + Kapton flex circuits
- + Cu traces + Au bond pads + wire bonds
- + Adhesives

Thermal Issues

Goal: Balance structure as much as possible

Problem: CTE for Be: 9×10^{-6}
CTE for Si: 2×10^{-6}
CTE for Cu/Ka: 23×10^{-6}

Sol'n (I): "Dummy" traces on flex project thru opp. side

- ...but CCDs still not thermally matched

Sol'n (II): Thick (200μm) adhesive pillars take up CTE mismatch

- even so...unsupported ladders ~100μm on cooldown

Sol'n (III): Clamp ladders to support structure w/blocks

$< 1\mu m$ *flex when cooled*

- ...but there are still local temp. gradients!

Sol'n (IV): Allow 1 dof (longitudinal) to take up differences

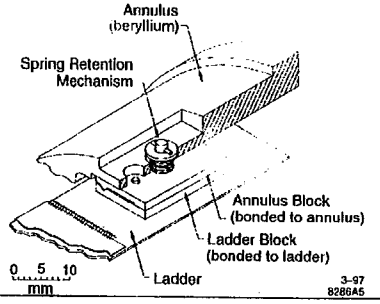

Mounting in SLD

Goal: Decouple vertex detector from machine

- Detector mounted off central beam pipe via 3pt. kin. mount
  Central beam pipe suspended from drift chamber
  3pt clamps w/adjustable jacks allow transverse adjustment
  → can tune VXD bkgds *in situ*
- Rest of beam pipe inside SLD "floats" between bellows
- Synch. rad. masks and outer beam pipe hung from FF quads

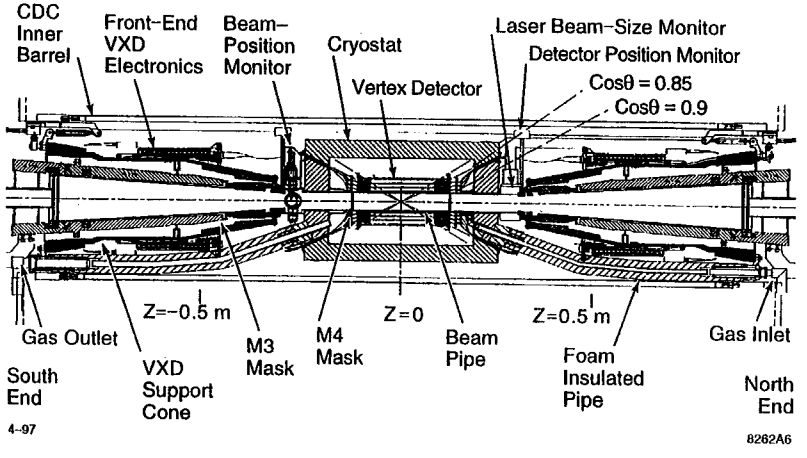

Data Flow

Goal: Readout 300MB at up to 2Hz, reduce to < 100kB

- **Solution: Digitize at front-end, sparsify at back-end**

  960 Mbit/sec raw data per frontend board (× 16 boards)

  Transmit 1.2 Gbit/sec/board via optical fiber + Glink

  Hardware cluster edge-finding + filtering

  1 CPU/back-end (Motorola 68040 @ 66MHz)

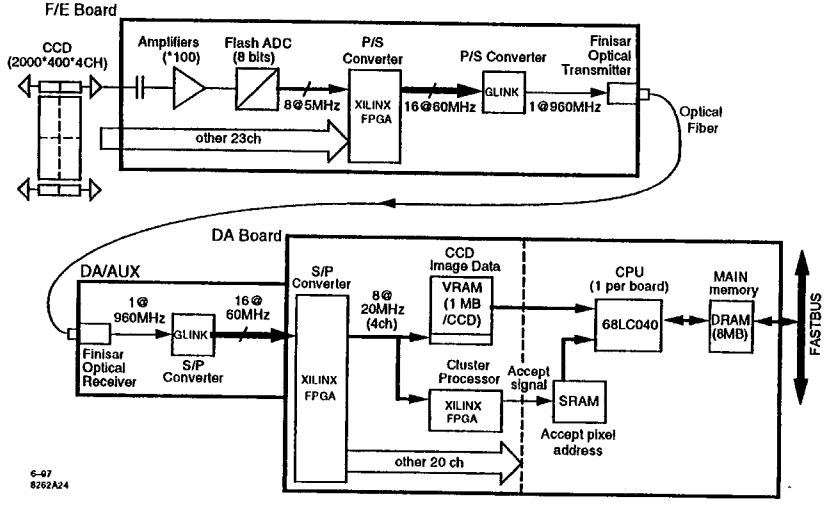

Data Acquisition Issues

Data Reduction

- **Cluster Processor (CP):**
  - Form 2×2 pixel filtered kernel
  - If above threshold, look for trailing edge
  - Once trailing edge is found, tag cluster, pass to CPU
  - Implemented via Xilinx FPGAs

Resource Allocation

- **Prioritize tasks:**
  1. Examine accepts from CP, save ROIs into memory
  2. Select pixels over threshold from ROI
  3. Assemble packets (26/event) into full event
  4. Sort by channel and CCD address, eliminate duplicates

476

Subtleties

- **Very limited memory up front**
  - Can store only $\sim \frac{1}{4}$ CCD full raw data
  - Cannot handle worst-case scenario
  - Data overrun cannot be prevented (only detected!)
  - Events can overlap and share packets (i.e., pixels)

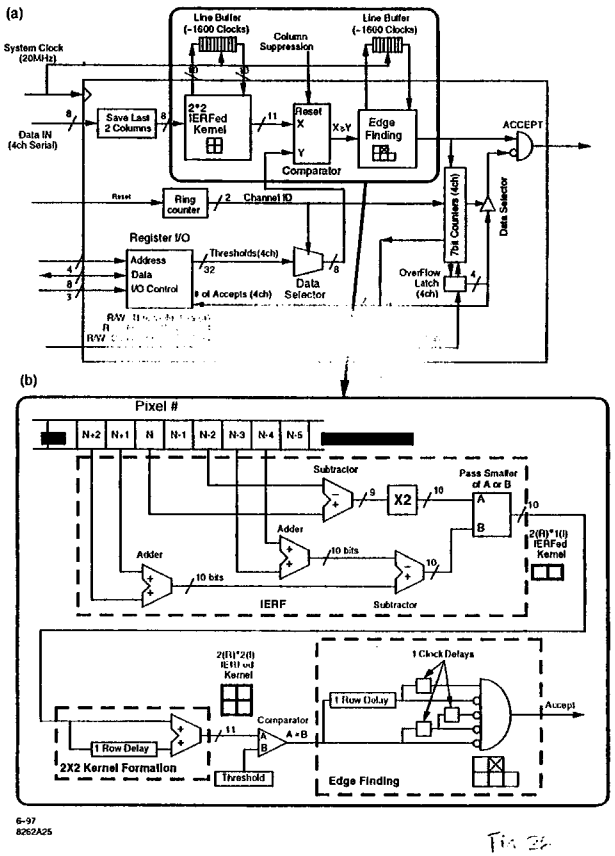

6-97
8252A25

Fig 2a

• Final internal alignment from tracks in all events

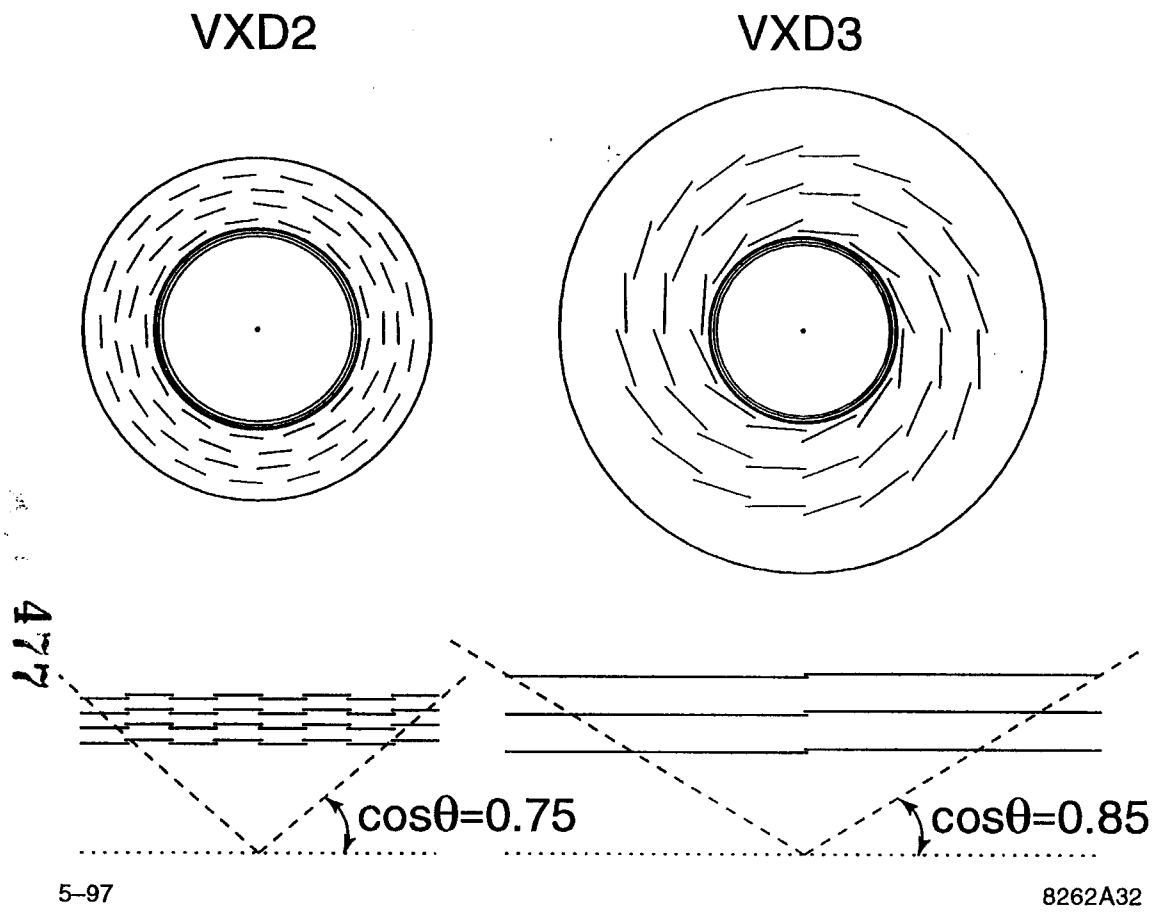

• Internal

"Shir
Lin
u

"Dou
Li
h

"Tripl
Lin
@

Derive "intrinsic resolution" from these comb.'s

Optical Survey Goals

MIT Group

- **Align detector well enough for track-based alignment**
  Need ~ 20μm precision overall
- **Determine complex geometric shapes**
  CCD shapes, gravity sag

Optical Survey Data:

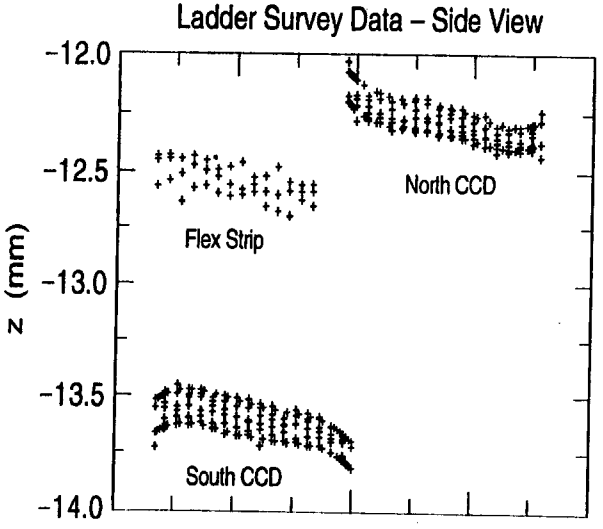

5-97

8262A8

Fits to CCD Shapes

all dimensions in mm · note scale differences

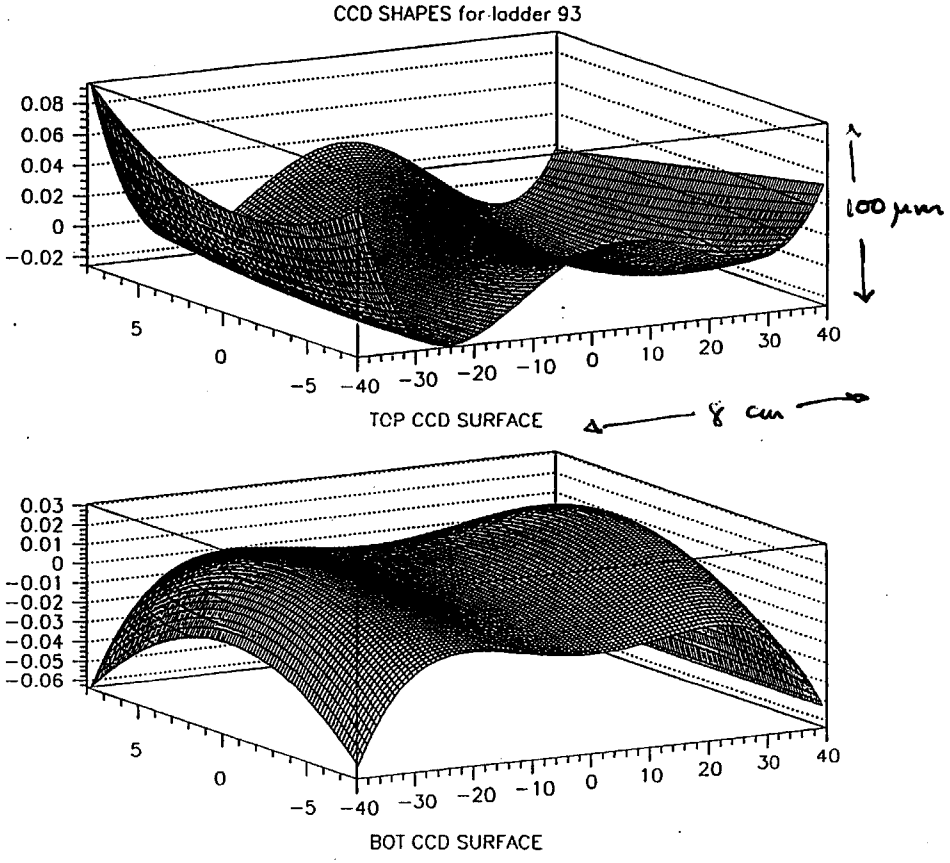

Optical Survey Results

- **Gravity sag:** up to 30μm correction/CCD
- **CCD shapes:** up to 50μm correction/CCD
- **Thermal corr'ns:** $\sim$ 50μm relative (Be/Si)
- **Precision:** 17μm $r\phi$. 14μm z
- **Systematics:** 20-30μm assembly repeatablility

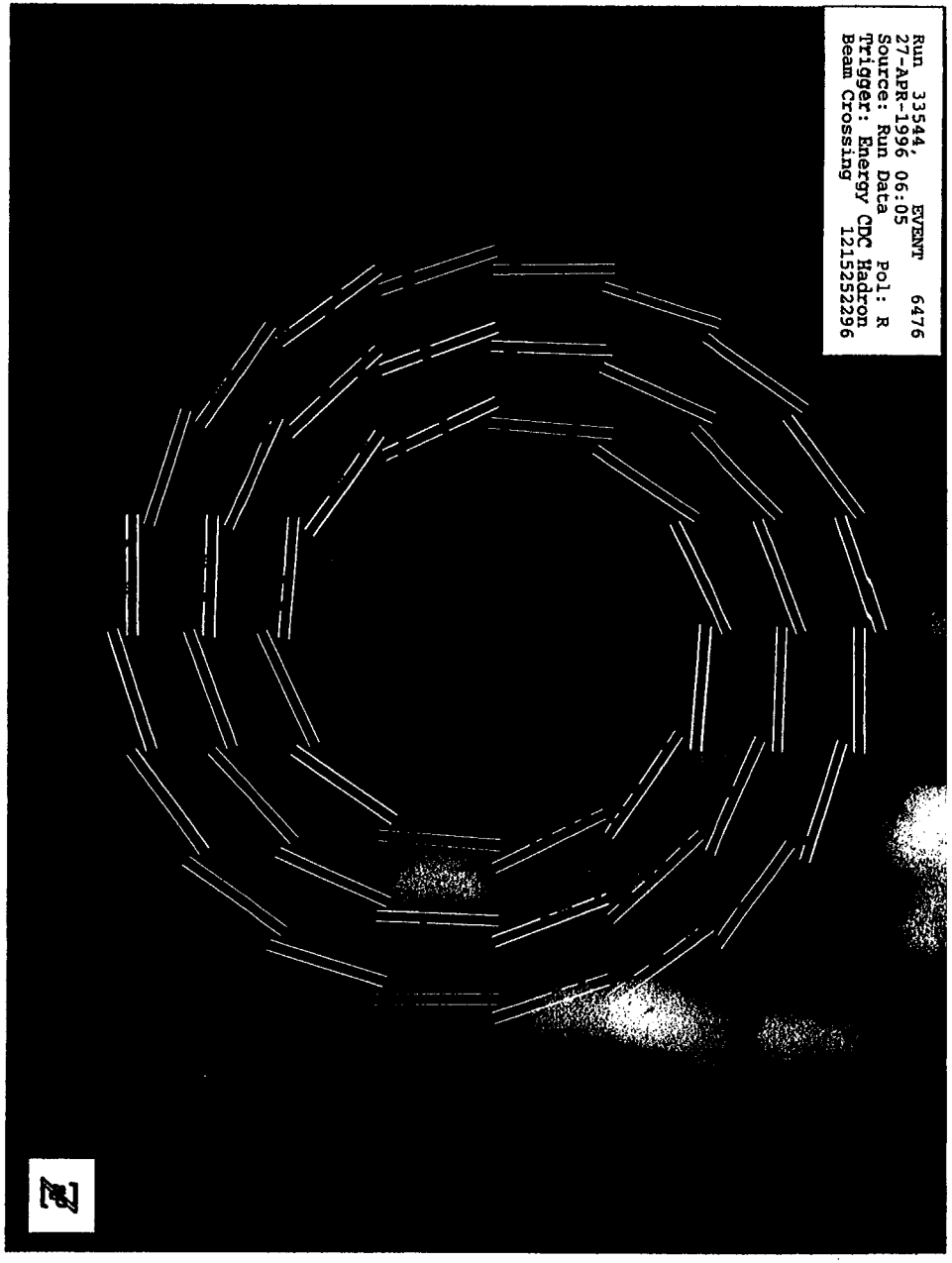

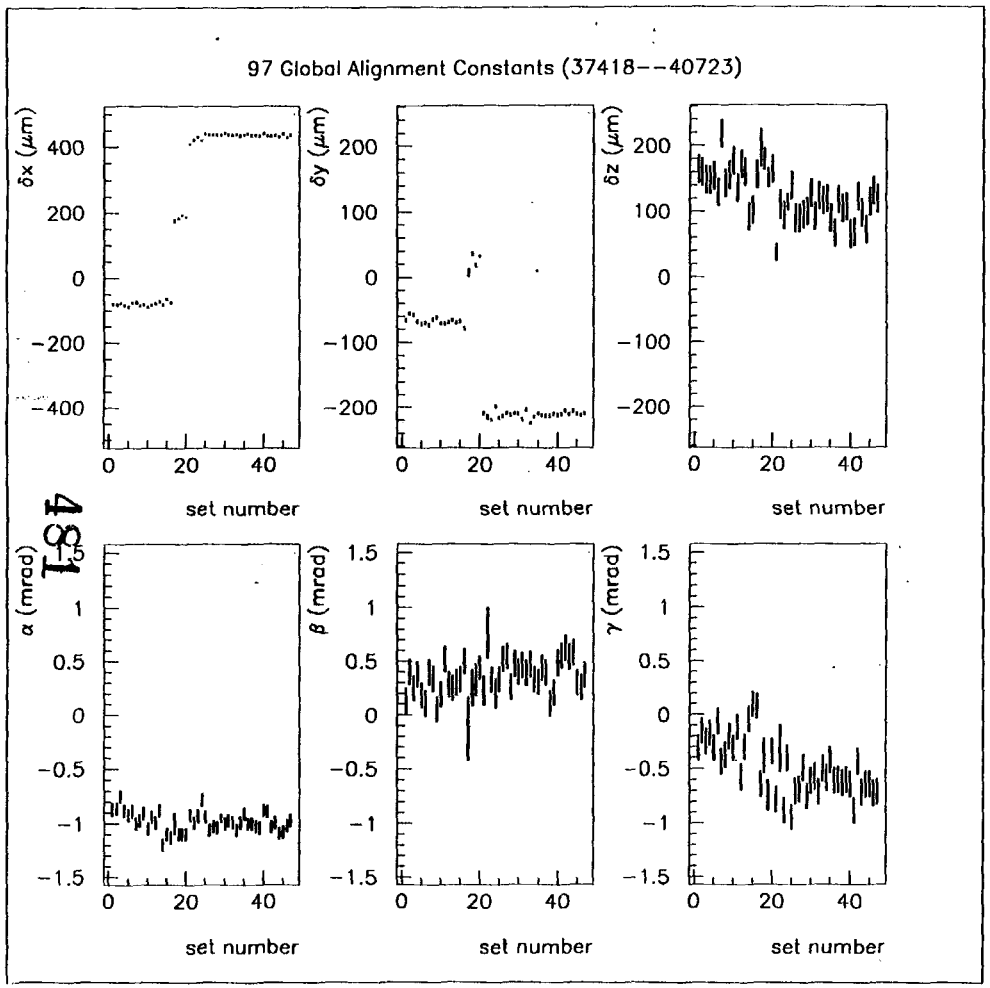

Detailed Alignment

D. Jackson et.al

- **Goal**: Determine location and orientation of all 96 CCDs:

  (3 translations + 3 rotations) × 96 = 576 parameters

  Need ~ 5μm precision (!)

- **Track-based alignment**: Determine local geom. w/ VXD alone

  Use track residual fits from vertex multiplets.

  Use MC + ideal geometry to determine CCD weights.

  Solve multiple coupled equations with matrices:

$$\begin{bmatrix} w_{ij} & \cdots \\ \vdots & \end{bmatrix} \begin{pmatrix} \delta x_i \\ \vdots \\ \delta\alpha_i \\ \vdots \end{pmatrix} = \begin{pmatrix} c_j \\ \vdots \end{pmatrix}$$

"Weight Matrix" CCD displacements Residual Fit Coeff.s

- Invert W and solve for $(\delta x_i, ..., \delta\alpha_i, ...)$

  (576 x 1520) matrix inversion! Fortunately most $w_{ij} = 0$

  Need to account for correlations in data, linear approximations,...

- **Add more information**:

  $Z^0 \to l^+l^-$ data

  VXD3/drift chamber matching redux

Intrinsic Resolution

- Spatial resolution derived from hadronic event track residuals
- Intrinsic CCD resolution $\sim$ doublet, triplet resolution
- Single-hit spatial resolution follows from geometry
- **Results:**

$$\text{Doublet } r\phi \;=\; 6.0\mu m/\sqrt{2} \;=\; 4.3\mu m$$

$$\text{Doublet } rz \;=\; 6.3\mu m/\sqrt{2} \;=\; 4.4\mu m$$

$$\text{Triplet } r\phi \;=\; 5.0\mu m/\sqrt{1.5} \;=\; 4.1\mu m$$

$$\text{Triplet } rz \;=\; 5.3\mu m/\sqrt{1.5} \;=\; 4.3\mu m$$

- **Significantly better than VXD2** ($\sim 5.5\mu$m)
- Unlikely to improve much (some small gains from final alignment)

Doublet and Triplet Residuals

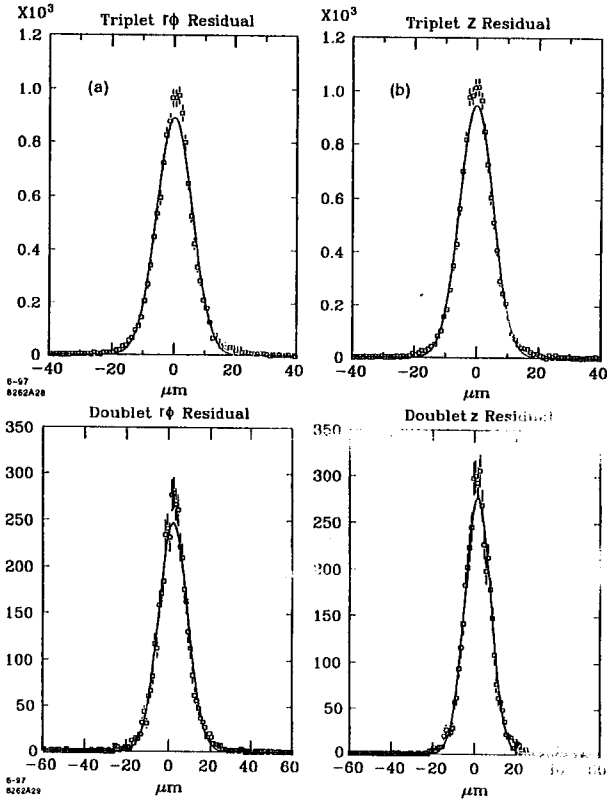

Impact Parameter Resolution, cont'd

- Low $\overline{p}$ end from track imp. params wrt beam: $\rightarrow$ *beam positions.*
- Dominated by multiple scattering and lever-arm
- Roughly 2X improvement seen.

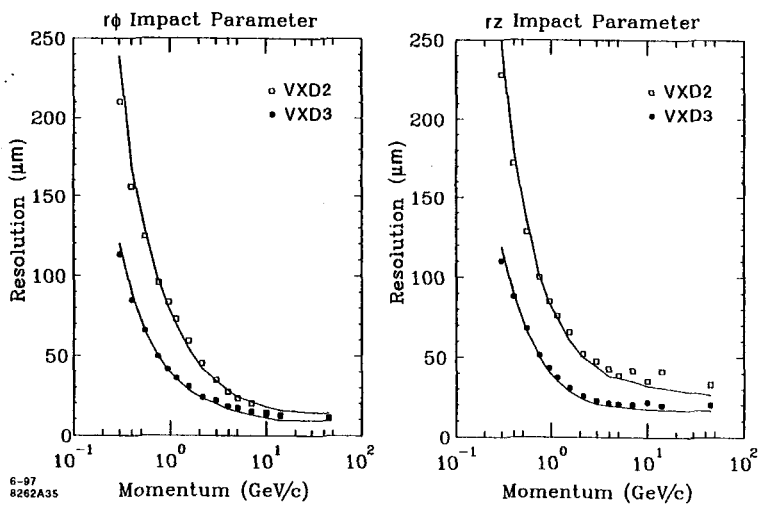

Lessons Learned

- Screening devices very important (20% failed)...QC!
- BeO ladders fragile, substrates crack, traces irregular
- Many delicate assembly connections...avoid Au flash!
- EM pickup into frontend electronics
- Optical survey *very* useful
- Alignment will take longer than you think

Dense Optical Interface Module for CDF – Design, Implementation, and Prototype Performance

M.L. Chu,[a] Y.C. Liu,[a] P.K. Teng,[a] M.T. Cheng,[b] M. Chertok[c]

[a] Institute of Physics, Academia Sinica, Taiwan
[b] Fermi National Accelerator Laboratory, Batavia, Illinois
[c] Texas A&M University

Abstract

The Dense Optical Interface Modules are general high speed communication links designed for the readout system of the CDF Upgrade Silicon Vertex Detector (SVXII). A 9-channel link consists of a transmitter (TX) module which converts electrical differential input signals to optical outputs, an intermediate multi-mode optical fiber ribbon cable, and a receiver (RX) module which senses the light inputs and converts them back to electrical signals. The targeted operational speed is 53 MHz, and higher rates can be achieved. The packaged TX and RX modules have embedded custom-designed laser diode arrays and photo diode arrays, as well as driver and receiver integrated circuits. These compact modules provide a good solution to data readout and interconnection problems common in future collider experiments. This article outlines the design goals, implementation methods, and prototype test results of these modules.

1 Introduction

High speed data readout modules and transmission links are crucial components for modern particle detectors. These devices normally have to be compact, low-mass, and capable of transmitting data at high speed without too much attenuation or error occurences. They also have to introduce very low electromagnetic interference (EMI) and be able to endure reasonable amount of irradiation after long periods of data-taking runs. Considering all the above factors, there are few commercially available products that meet most of the requirements for particle experiments.

The Dense Optical Interface Modules (DOIM) [1], [2], are custom-designed for the readout system of the CDF Upgrade Silicon Vertex Detector (SVXII). It is a cost-effective solution to the data readout tasks that meets most of the above stringent requirements.

As shown in the layout diagram in figure 1, a full DOIM communication link includes three parts - the transmitter (TX) module, the intermediate optical fiber

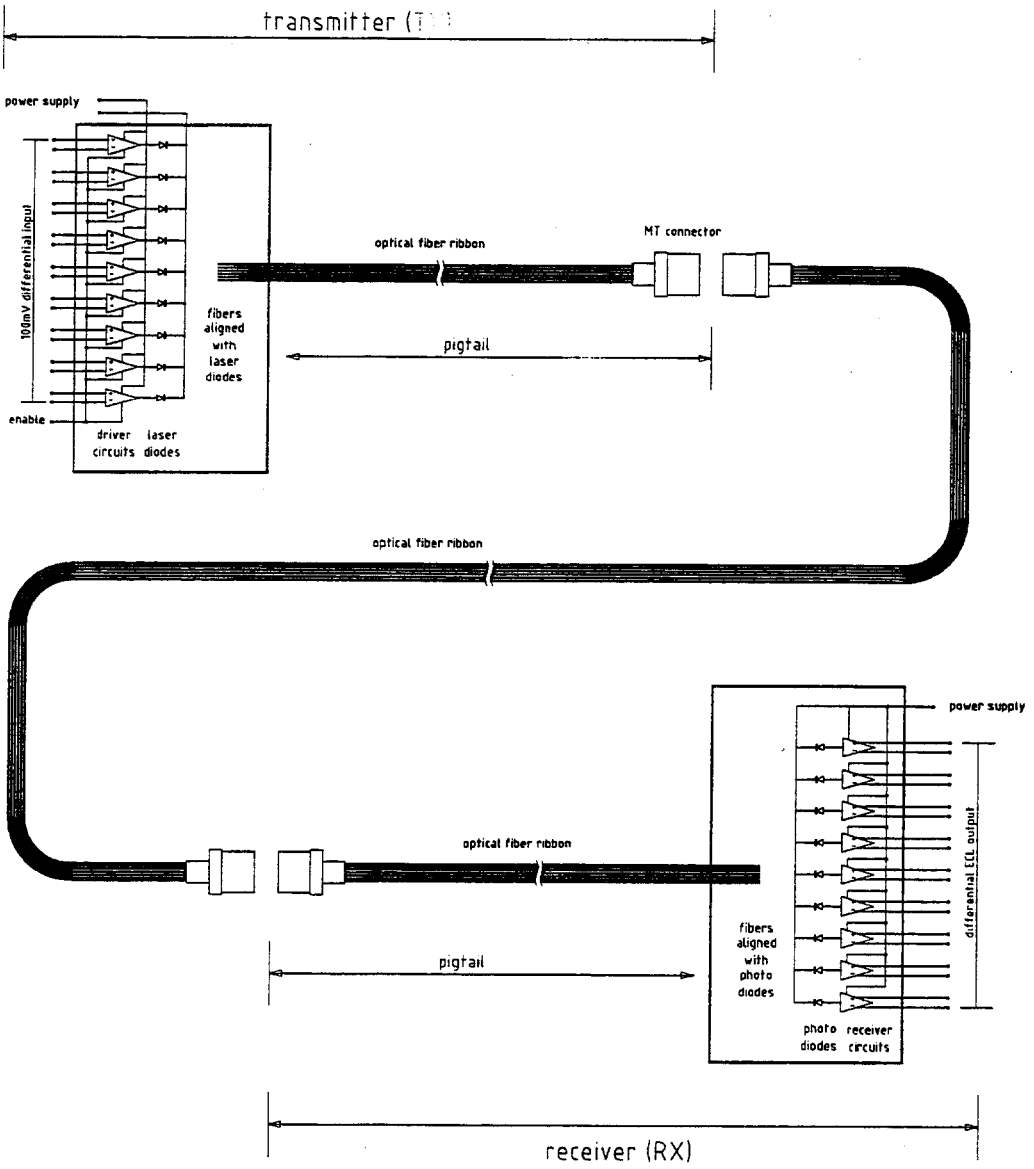

Figure 1: Layout of a DOIM data link.

ribbon cable, and the receiver (RX) module. It will take totally 360 such links to read out the whole SVXII detector.

The TX module encapsulates the driver integrated circuit which conditions the input differential electrical signals [3], and the 9 channel laser diode array which converts the signals to light outputs to be sent out via the optical fiber ribbon.

Between the transmitting and receiving ends, we use 9-channel commercial multi-

Table 1: Transmitter Module Design Parameters

Parameter	Typical	Unit
Input Signal	> 20 (differential)	mV
Data Rate	53	Mbit/sec (per channel)
Optical Output Power	> 200	μW (per channel)
Rise Time	< 2	ns
Power Consumption	< 1.2	W/module
Duty Cycle	50	%

Table 2: Receiver Module Design Parameters

Parameter	Typical	Unit
Data Rate	53	Mbit/sec (per channel)
Output Signal	differential ECL	
Photo Diode Responsivity	1	A/W
Rise Time	< 2	ns
Power Consumption	< 1.6	W/module
Input Threshold	40	μW (per channel)

mode fiber ribbon cables to guide the light outputs from the TX modules at the inner layers of the detector to the second stage of the data acquisition system that is external to the detector. These are $62.5\mu m$(core)/$125\mu m$(cladding) fibers operated at a wavelength of 1550 nm. For ease of deployment, small segments of fiber ribbon *pigtails* are attached on both TX and RX modules, with one end of the fiber cable terminated with standard MT(TX)/MTP(RX) type connectors, and the other end aligned with the diode arrays on the module substrate.

The RX module contains a 9-channel photo diode array (PDA) as light sensors and the transimpedance amplification and decision integrated circuits.

2 Design Specification

The specification is separated into two parts for the TX and RX modules. The operational parameters were chosen based on the detector application requirements and the availability of various technologies. Tables 1 and 2 list the design parameters for either type of modules.

The power connection scheme for the TX is a bit more complicated than the RX module. A separate supply level, *Vld*, are provided for the laser diode arrays as the common to all cathodes. The driving scheme for the laser diodes is as shown in figure 2. This is required so that we can adjust the laser driving currents for optimal

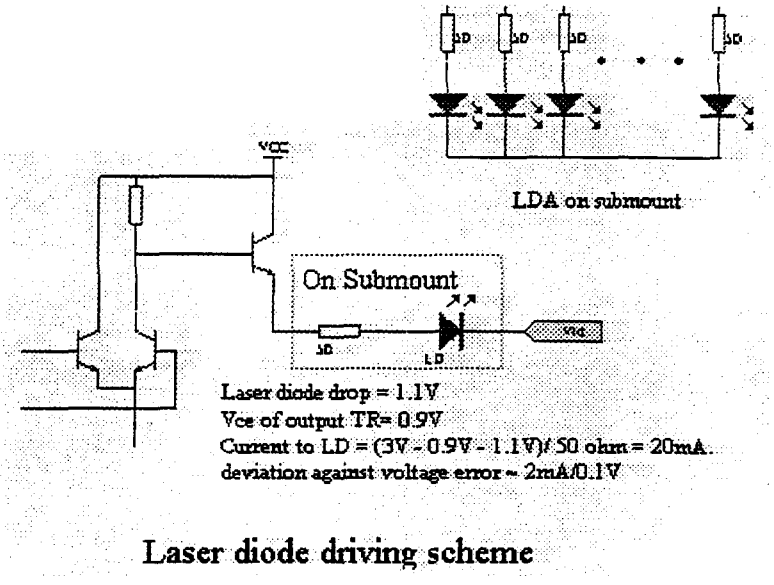

Figure 2: Driving scheme of the TX laser diode array.

light outputs from the TX modules. After years of running in the high radiation environment, we expect the light output levels to be gradually degrading. By having a separate and adjustable supply level for the laser diodes, we will have the capability to raise the light output levels back to acceptable ranges later on.

3 Component Implementation

Various issues have been taken into consideration when deciding on which technologies to adopt for making the prototype DOIM Modules. The most important factors are,

- High operational speed
- Compactness
- Radiation hardness
- Power consumption

The following section summarize the implementation methods of each component.

3.1 Driver and Receiver Integrated Circuits

The prototype driver and receiver ICs were implemented successfully with a BiCMOS/BiPolar technology, based on its high speed capability and reasonable endurance in radiation environment compared to CMOS technologies. Production chips have been fabricated based on this successful design.

3.2 Laser and Photo Diode Arrays

The LDA technology used for the current version of the TX modules is the edge-emitting ridge-waveguide $InGaAsP/InP$ quantum well lasers. The pitch between lasers is 250 μm, and we make multiple-channel arrays and simply pick up the ones that have 9 consecutive functioning channels. Before module assembly, every laser is required to have at least 700 μW output power to leave enough margin for coupling losses expected during the alignment process with the optical fibers.

For the PDA in the RX module, we used $InGaAs/InP$ PIN photo diode arrays. Again, the pitch between diodes is 250 μm.

Both the LDA and PDA technologies are developed and fabricated for the CDF SVXII application at the Telecommunication Laboratories, Chung-Li, Taiwan.

New technologies like Vertical Cavity Surface Emitting Laser (VCSEL) is being evaluateded for possible replacement of the currently used edge-emitting diodes. This can further improve on light coupling, laser driving current reduction, and array fabrication yield.

4 Module Assembly

To package the various components into functioning TX and RX modules, we started by bonding the laser and photo diode arrays onto their submounts. After the array DC and burn-in tests, the submounts were installed on the ceramic module substrate.

On the other hand, the driving and receiving integrated circuit chips are bonded on the substrate and tested separately.

Then, the optical fiber ribbon cable is stripped at one end to expose the fibers. The fibers are then aligned with the diodes on the LDA or PDA, and hold in place by silicon V grooves as shown in figure 3.

Finally, plastic covers are placed on the module substrate to secure the components mounted on it. This will make the whole module more hermetic. Figure 4 shows the dimensions of the finished prototype TX and RX modules.

5 Prototype Tests

The first prototype of the fully packaged TX and RX module came out in the Spring of 1997. Various tests have been performed on these modules to establish their basic operational characteristics and to understand their behavior under temperature and humidity fluctuations and their survivability in radiation environment.

5.1 Basic Characteristics

The configuration of the test set-up for measuring the basic operational characteristics for the TX modules is as shown in figure 5. The module is powered up with two

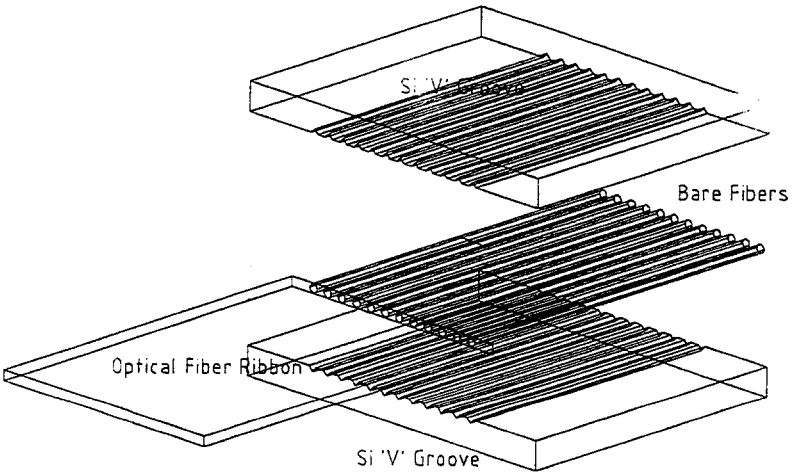

Figure 3: The optical fibers are hold in place by silicon V grooves.

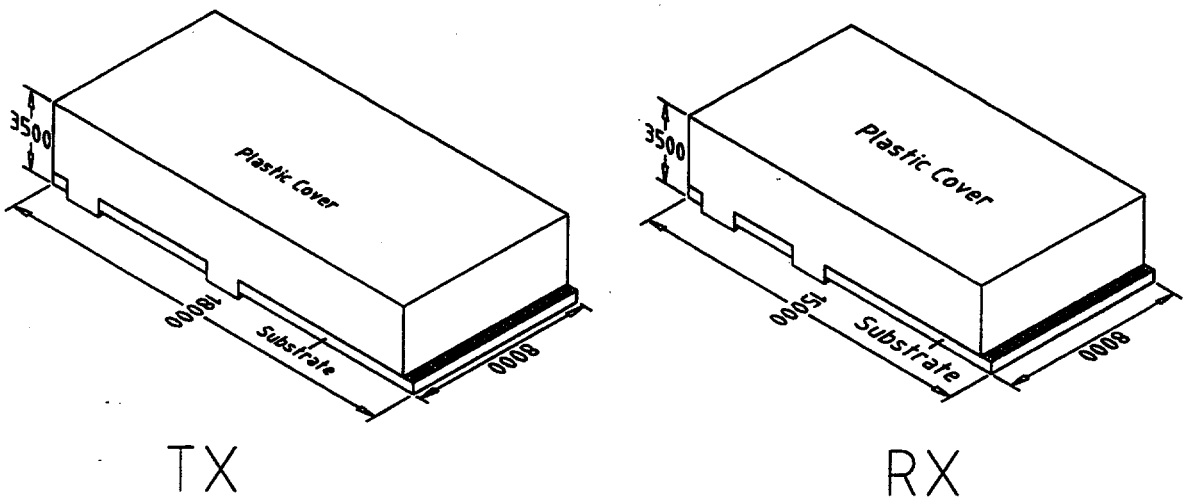

Figure 4: Finished TX and RX module dimensions (unit : μm) , after the module plastic cover is placed.

separate power levels, one for the driver circuit (Vcc - 1V) , one for the laser diode array (2V, or 3V below Vcc). Input signals are fed to all 9 channels, so they are switching simultaneously. The opitcal power levels and waveforms for each channel were converted to electrical signals by the Tektronix P6703B 0/E converter and observed on a digital oscilloscope. Normal channels that meet the design specification would have peak output power greater than 150-200 μW. A typical output waveform

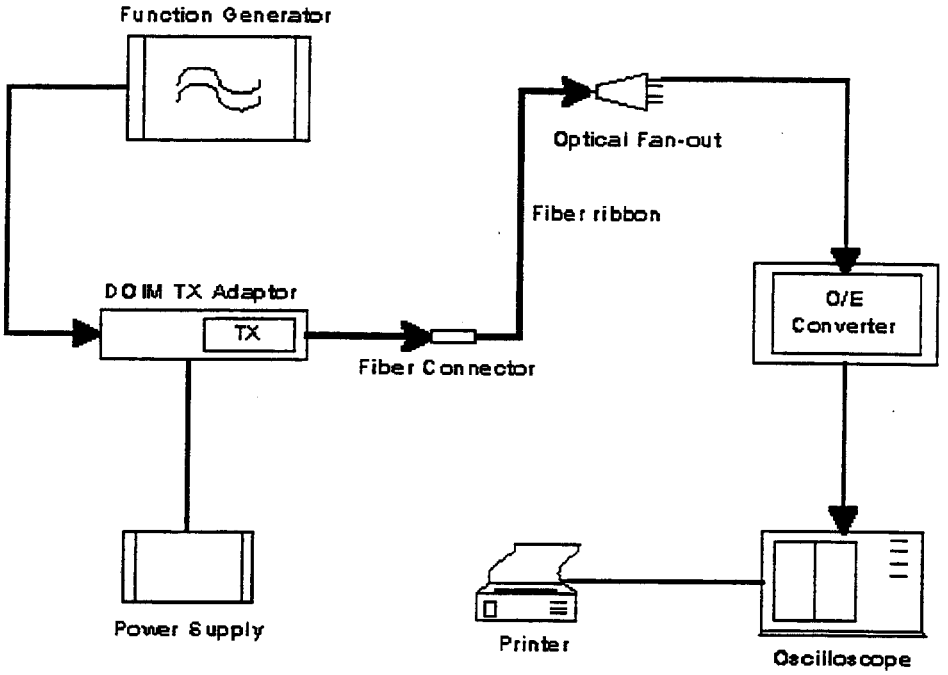

Figure 5: Transmitter module basic operating parameter test set-up.

is shown in figure 6.

For the RX module, we used a calibrated TX module as the input light source and observed the differential ECL output waveforms. A typical RX output is shown in figure 7.

5.2 Bit Error Rate Test

A crucial performance parameter for data communication modules is the Bit Error Rate (BER), which is defined as the number of bits decoded in error versus the total number of bits received. The DOIM design specification requires that the BER be $< 10^{-12}$.

To measure the BER for the prototype DOIM TX-RX link, we used the Fermilab custom-designed Bit Error Rate Tester (BERT) [4]. The test set-up is as shown in figure 8. Both random and alternating data patterns were generated at the TBERT module, and transmitted to the RBERT module via a full DOIM TX-RX link. The data received at the RBERT end were then compared to the pattern originally sent to locate any burst of errors.

The test was conducted for more than 7 days with both data patterns, before the first error came about on one of the 9 channels. This corresponds to a BER of better than $< 10^{-14}$, two order of magnitude better than what the design specification required.

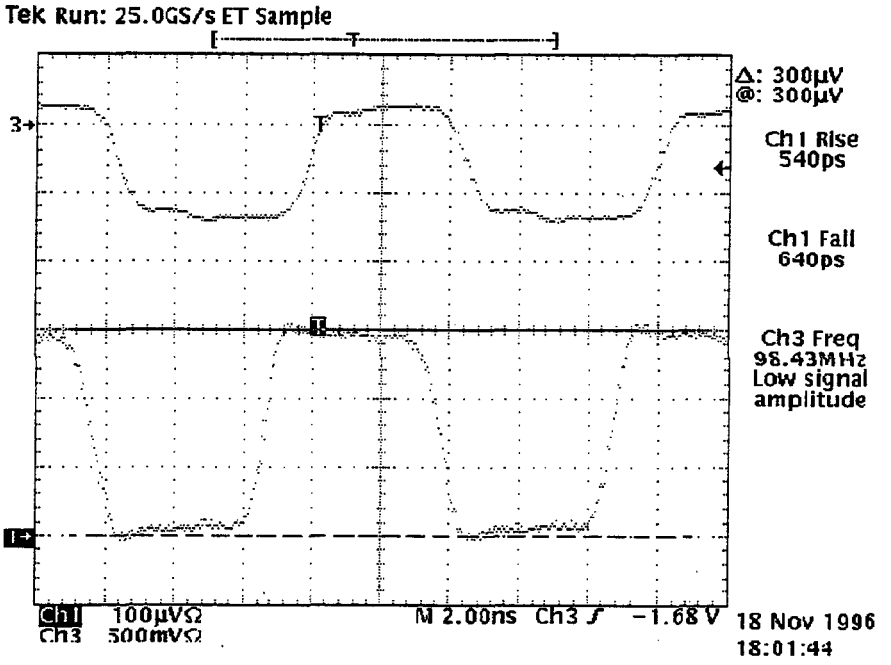

Figure 6: Typical transmitter optical waveform, as shown on Ch1 of this captured digital scope display. Note that this module is operated at 98 MHz to test its capability at higher frequencies.

5.3 Power Consumption

For the TX module, the power consumed by the driving circuits is relatively constant independent of the data patterns. The power drawn by the laser diode array depends on the adjustable Vld supply level and the data pattern. The worst case senario is when all 9 lasers are on all the time. A typically averaged range is for a duty cycle of 50%, at which a total power of 1W is consumed by the whole module (9 channels). The power scheme for the RX module is simpler. There is only one Vcc supply. The power consumption is measured to be 1.6W per module. The above measured power dissipation rate is well within the power budget required by the design specification.

5.4 Radiation Hardness

For the projected 3 years of running periods for the Fermilab Tevatron Run II, the DOIM TX modules are expected to receive an average total dose of close to 250 KRad. To establish their functionality under radiation environment, we have carried

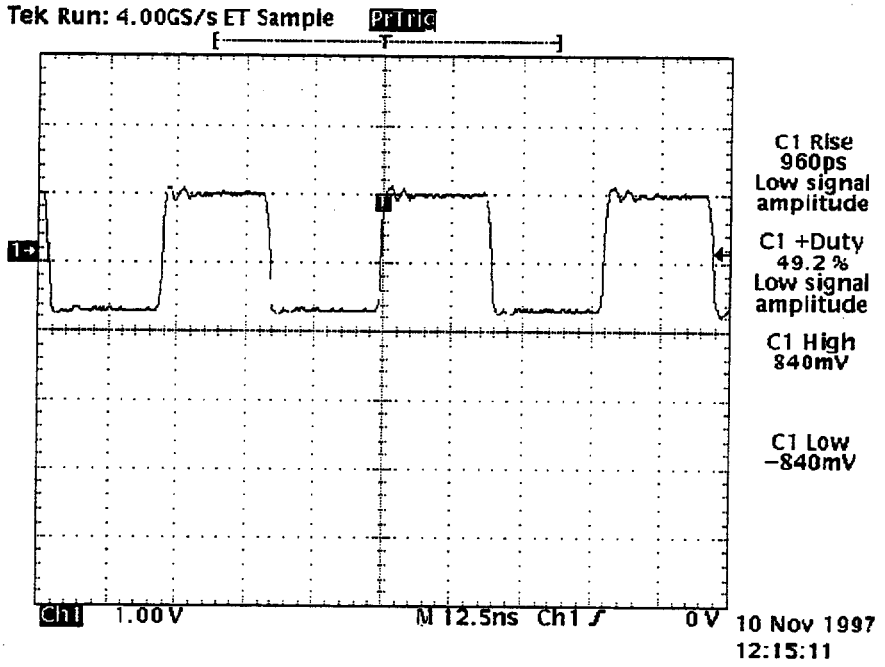

Figure 7: Typical receiver differental output waveform.

a few tests at the Fermilab Booster area with 8 GeV proton beams.

The first test on just the BiCMOS/BiPolar driver circuit (July 1997) showed no observable degradation of the switching characteristics on the chips up to a total dose of 1 MRad.

We also subjected 1 fully packaged prototype TX module in the same beam for up to 1.5 MRad. The module was powered up and fed with 50 MHz input signals during irradiation, and the output waveforms were monitored periodically throughout the irradiation. For the 4 consecutive runs as shown in figure 9, we observed that the light output decreased consistently by 25% after roughly every 250 KRad of accumulated dose, and the degradation corresponded roughly to the time when the beam swept through the module. This is a combined effect since degradation in output came from both the LDA in the module and the darkened fibers.

After the 1.5 MRad total radiation dose, the TX module still had output power level beyond that is required by the RX switching threshold/sensitivity. Therefore, the prototype modules are capable of dealing with the 250KRad in the Run II environment.

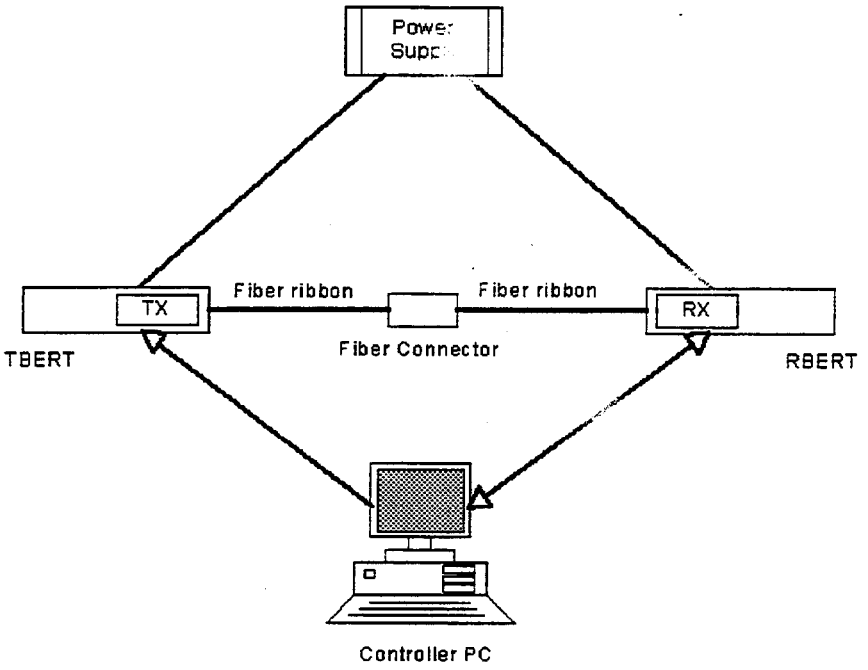

Figure 8: Bit Error Rate test set-up.

5.5 System Integration

The DOIM TX modules are to be installed on the Port Cards [5] of the SVXII detector data acquisition system. These are custom-designed boards that control the front-end readout chips at the silicon sensors and send the data out via the 5 DOIM TX modules on each Port Card.

On the other end, the RX modules are located on the Fiber Interface Board (FIB) [6] which are installed in racks outside the whole detector structure. They translate the data from the differential ECL outputs from the DOIM RXs to TTL levels and transmit them out to trigger system and readout controllers.

The prototype DOIM TX-RX link has been tested with the prototype Port Card and Fiber Interface Boards. The full link has been demonstrated to be transmitting valid data from the front-end readout chip. This is a milestone for the successful implementation of the SVXII data acquisition system. Larger scale system integration test is currently underway.

6 Conclusions

From the various tests performed on the prototype TX and RX modules, we found that the DOIM design was sound and that the first implementation met the design

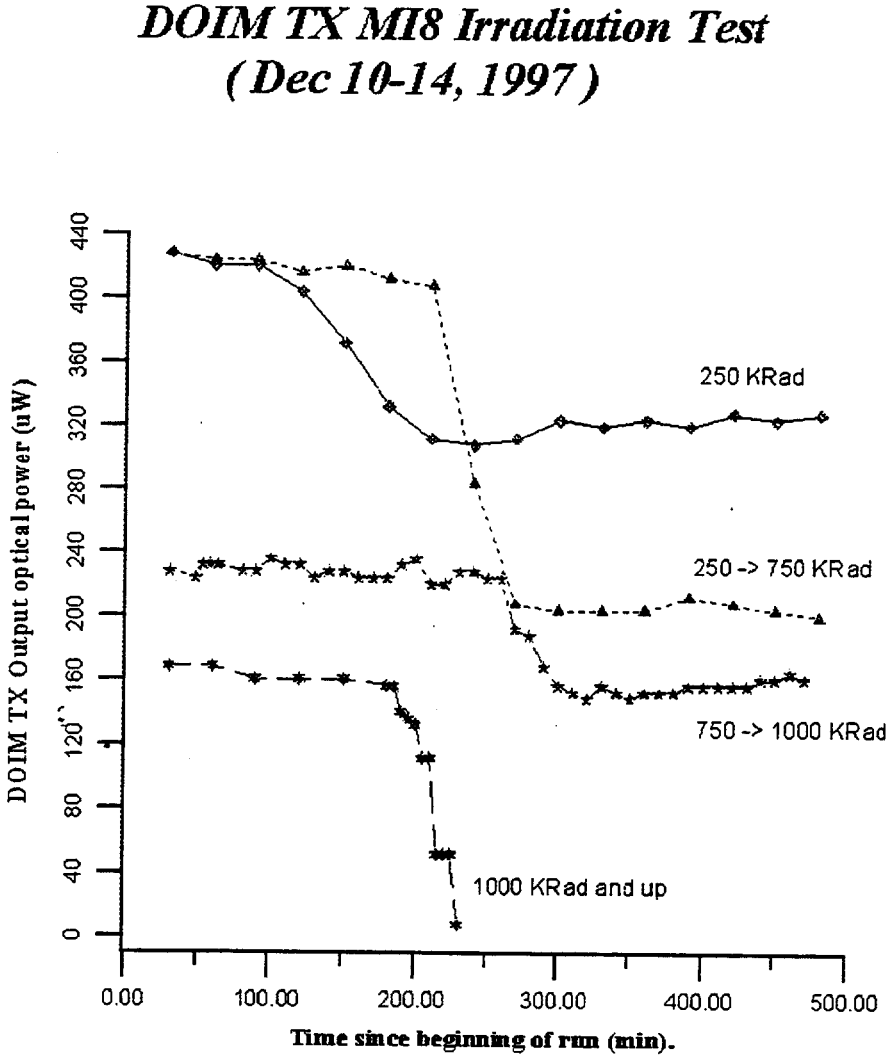

Figure 9: TX module 8 GeV proton irradiation test - Optical Output Power (μW) vs. Elapsed Time (min) during 4 runs, with accumulated dose for each run indicated on each curve.

requirements. The production process of these modules is currently underway, and full delivery for CDF SVXII application is expected by Spring of 1999.

We are currently exploring further improvement on TX laser diode optical output uniformity, by fine-tuning the alignment process. Production level burn-in and system integration tests are also in progress.

7 Acknowledgement

This project is supported by the National Science Council of Taiwan, Republic of China.

References

[1] M. L. Chu, M. T. Cheng, Y. C. Liu, *Dense Optical Interface Module (DOIM).* CDF Internal Note 3865 (Fermilab, IL, 1996).

[2] P. S. Chang, et al., *Dense Optical Interface Module for Silicon Detector Readout.* Nucl. Phys. B (Proc. Suppl.) 61B, 360-365 (1998).

[3] E. Barsotti, S. Zimmermann, *Low Current Differential Signal.* Fermilab Engineering Note ESE-SVX-950605 (Fermilab, IL, 1995).

[4] D. Husby, *BERT, Bit Error Rate Tester.* Fermilab Engineering Note ESE-SVX-950222 (Fermilab, IL, 1995).

[5] H. Gonzalez, K. Treptow, S. Zimmermann, J. Andresen, *Test Port Card.* Fermilab Engineering Note ESE-SVX-950808 (Fermilab, IL, 1995).

[6] K. Woodbury, *Fiber Interface Board (FIB).* Fermilab Engineering Note ESE-SVX-951010 (Fermilab, IL, 1995).

Pixel Detectors using MCM-D Technology

May 8th 1998

Peter Gerlach
Bergische Universität-
Gesamthochschule
Wuppertal

K.H.Becks
P.Gerlach

E.Beyne
P.Pieters
C.Truzzi

O.Ehrmann
J.Wolf

Workshop Pixel98

FNAL May 7-9th 1998

MCM-D, what's that ? (1)

- Thin film technology, integrating bus systems on a substrate
- Developement (a.o.) at
  - Interuniversity Microelectronics Center (**IMEC**, Leuven, Belgium)
  - Frauenhofer Institute for Reliability and Microintegration (**IZM**, Berlin, Germany)

497

MCM-D, what's that ? (2)

conductor layers

- Up to 5 copper layers:
  - magnetron sputtered
    up to 2 µm Ti/Cu/Ti
    ⇒ 10 mΩ/□
  - additive electroplating
    up to 5 µm Ti/Cu
- Minimal width and spacing
  15 and 20 µm
- Final metallisation:
  electroless
  5µm Ni:P/ 200nm Au

dielectric layers

- "Spin-on" polymer: BCB
  (Benzocyclobutene / DOW:CYCLOTENE™)
- Photosensitive
- Specific dielectric constant
  $\varepsilon_r = 2.7$
- Process temperatures :
  1h 220°C per layer
  last layer 1h 250 °C
- Thickness / layer 4 - 10 µm
- Via ∅ >20 µm, Pad 30µm

Structure of a Module **without** MCM-D

Example: DELPHI vertex detector pixel module (Raquette)

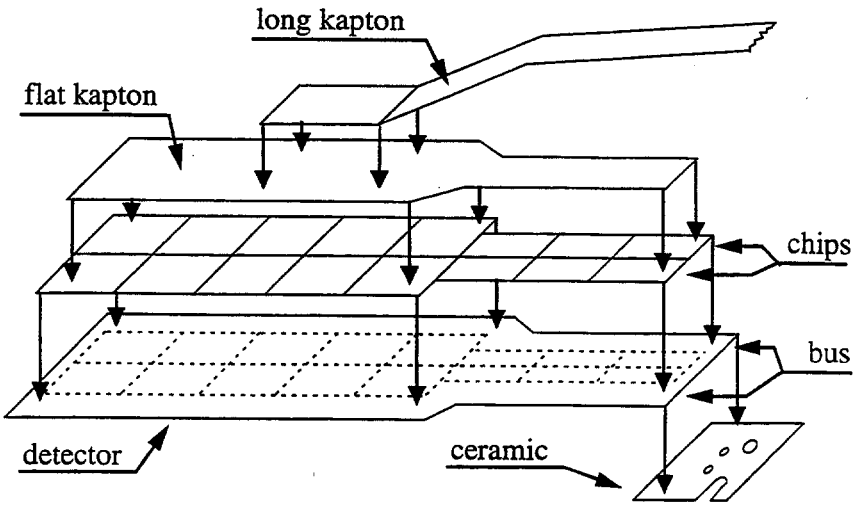

Structure of a Module **with** MCM-D

P.Gerlach — University of Wuppertal

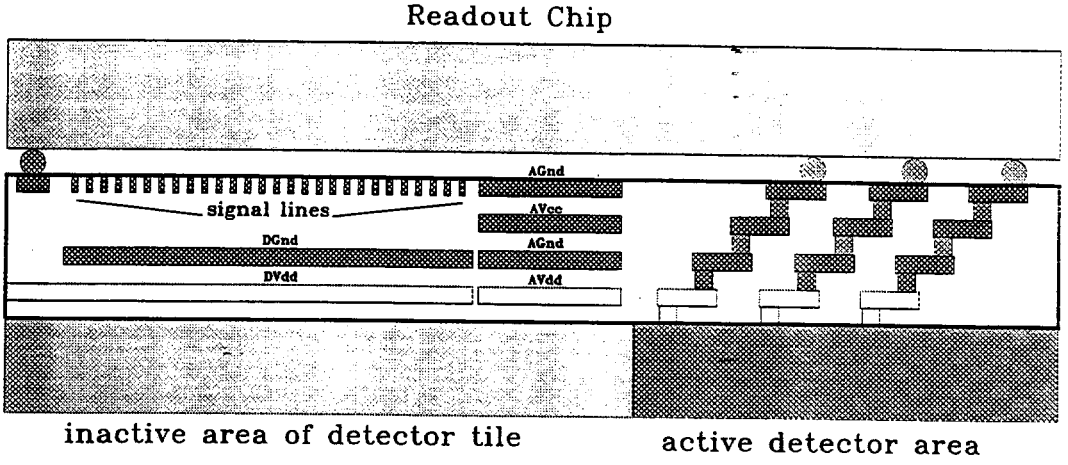

Cross-Section of a Bus System

P.Gerlach — University of Wuppertal

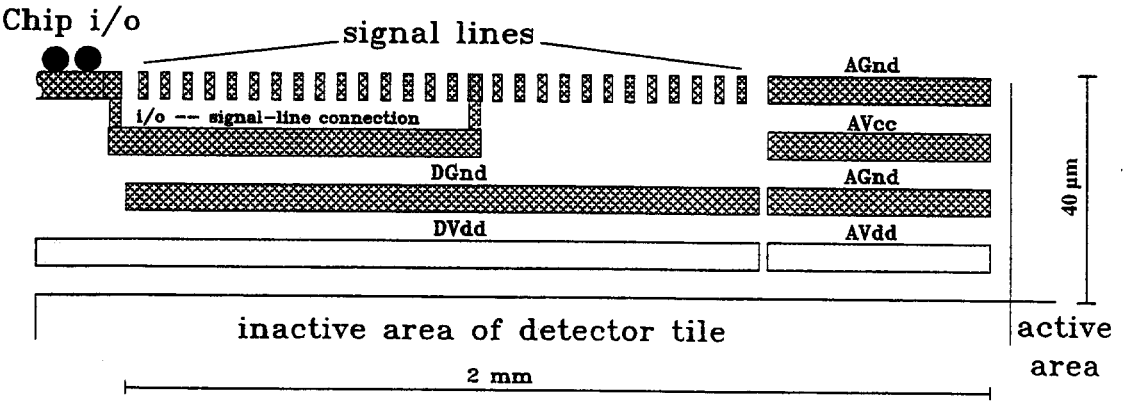

Top View of a Bus System

P.Gerlach
University of Wuppertal

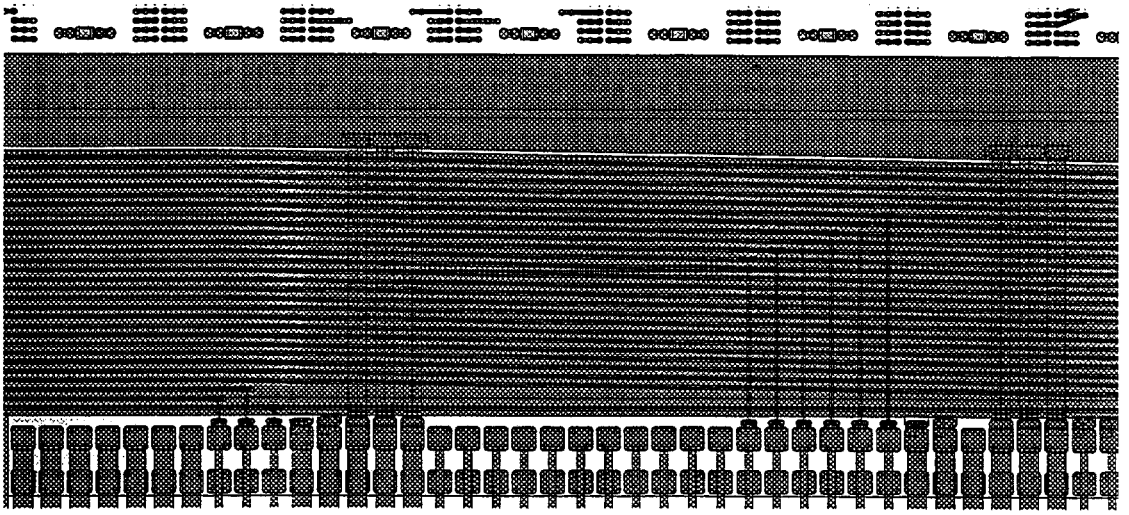

R&D Program

P.Gerlach
University of Wuppertal

- ☑ Geometric requirements
- ☑ Radiation hardness
- ☑ Bump-bonding tests
- ☐ Test on active silicon
- ☐ Demonstrator module

Performance of the Bus System (1)

Bus system for 8 readout chips

Signal-Bus:

A 7cm long bus made of microstrip-lines 20 µm wide with 30 µm spacing shows

- Z_0= 68 Ω
- Crosstalk < 3%
- Signal-attenuation < 4 dB (<1GHz)

Power Supply Bus:

Calculations

⇒

- Power loss < 150 mW
- Max. difference of potentials 100 mV

Performance of the Bus System (2)

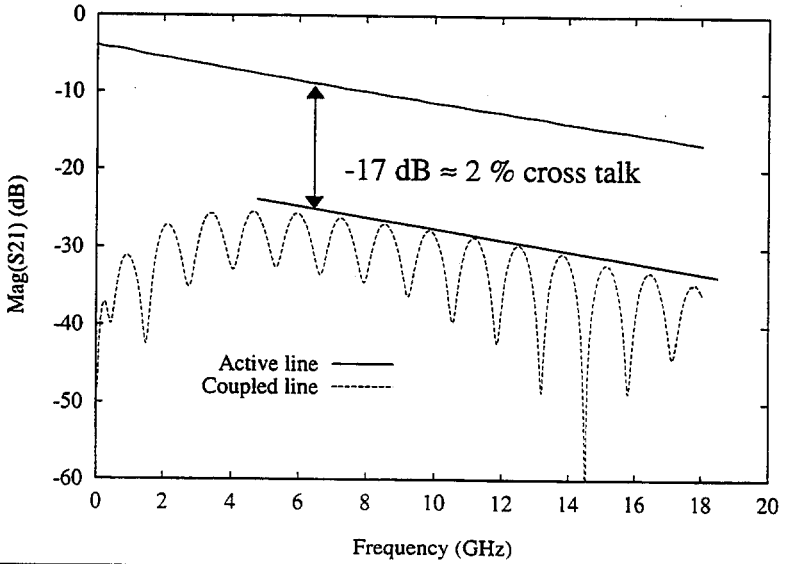

IMEC

Radiation Hardness (1)

- 10^{15} e^-/cm^2 at 40 keV cause a change in ε_{r_eff} of **2%**. (Irradiation by C.Becker, Univ.Dortmund)
- Irradiation of the same test-wafer with $5 \cdot 10^{14}$ p^+/cm^2 at 24 GeV protons causes a change in ε_{r_eff} in total of **3%**. (Irradiation at CERN)

⇨ *Due to absorption of moisture, a change in ε_{r_eff} of **1.4%** is expected.*

Radiation Hardness (2)

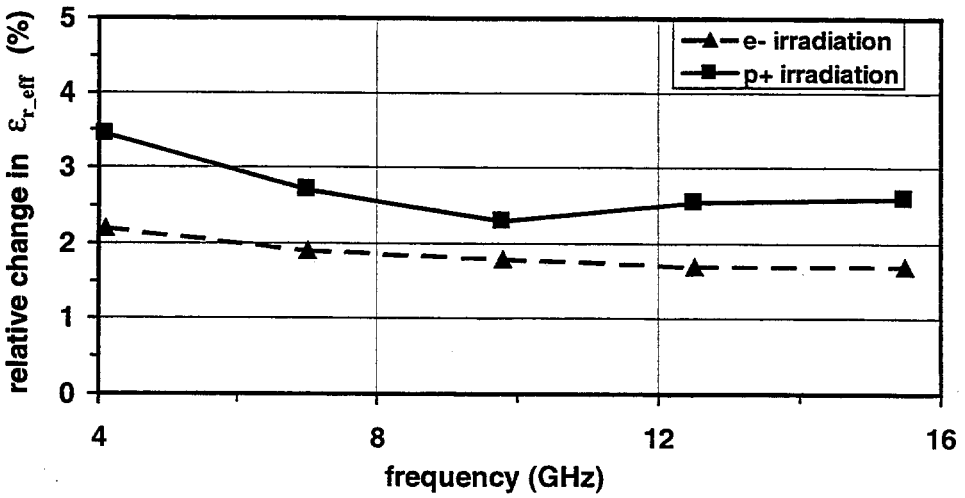

IMEC

Bump-Bonding Tests

- Two wafer layouts
  (detector and r/o-chips)
  with "daisy-chain" of bump connections
  (University of Bonn / IZM Berlin)
- 1.1 ·10^6 monitored vias with a diameter of 25µm indicating an error rate < $\mathbf{10^{-5}}$

Layout of a Feed-Through Structure

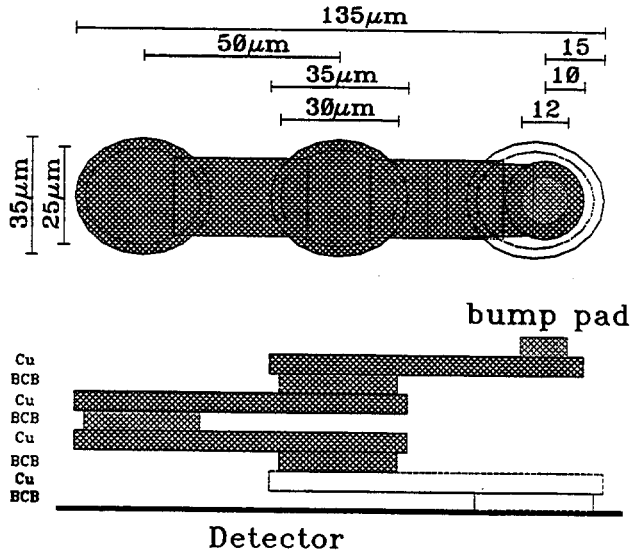

Cut through Bump Region

P.Gerlach University of Wuppertal

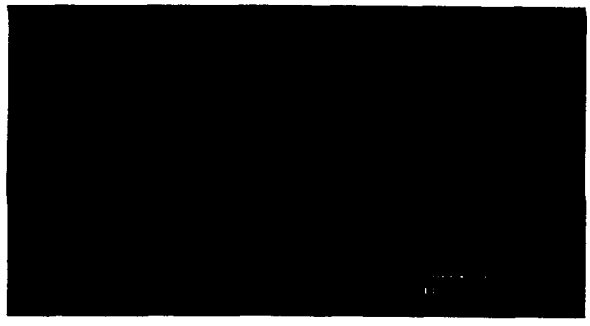

Photograph IZM

- Cross-section of flip chip bondet IC's on silicon substrate
- Bump pitch 50 µm
- 4 Cu layers and 5 Photo-BCB layers
  Photo-BCB: 5 µm thick, 25 µm vias

Feed-Through Structures

P.Gerlach University of Wuppertal

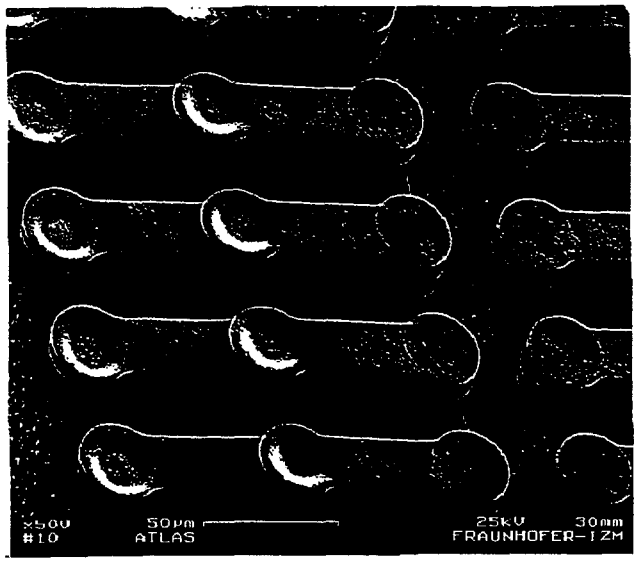

- Four copper layers
- BCB etched for better visualisation
- Measured defect rate
  $8.13 \cdot 10^{-6}$
  (9 defects in 1 105 920 vias)

Photograph IZM

Feed-Through Parasitics

P.Gerlach — University of Wuppertal

- Resistance:
  - 2µm Cu-Layer ⇒ 10 mΩ / □
  - 5 mΩ per Via
  - ⇒ 60 - 160 mΩ per feed-through
- Coupling Capacitance:
  - 20 - 40 fF between 2 adjacent feed-throughs

Photograph of IZM MCM-D Prototype

P.Gerlach — University of Wuppertal

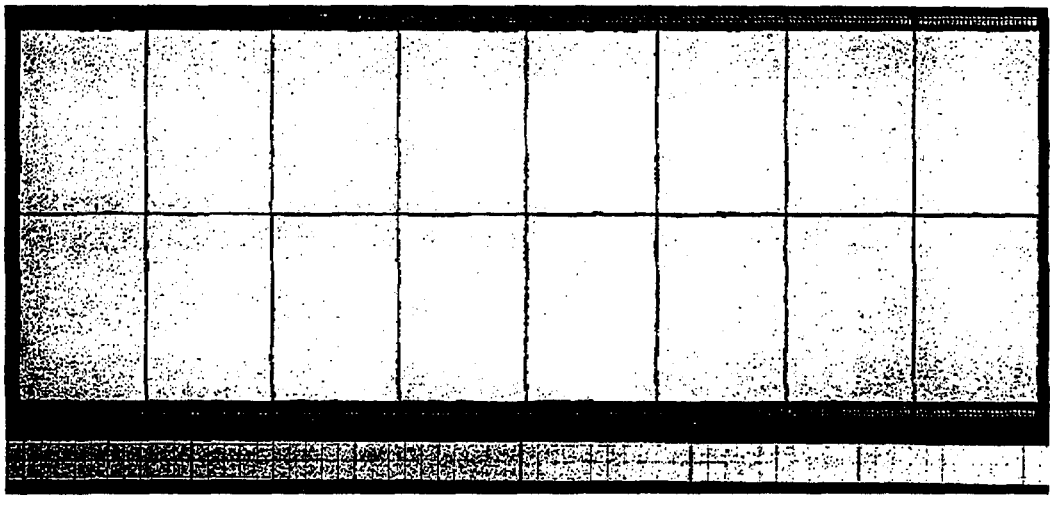

Multi Chip Module - Deposited Conclusions

radiation hard thin film technology

Up to **5 copper** layers

- Layer thickness up to **5 µm** (2µm Cu-Layer ⇒ 10 mΩ / □)
- Line width/pitch **20/50 µm**
- Impedance controlled

Benzocyclobutene (**BCB**)

- ε_r = **2.7**
- Layer thickness **4 to 10 µm**
- Via down to **∅ 25 µm** (~1mil)
  failure rate **< 10^{-5}**

In progess:

- Test on active silicon
- Demonstrator module

The CDF SVXII HDI and Long Cu-Kapton Flex Cables

Mark Bailey
New Mexico Center for Particle Physics
University of New Mexico
for the CDF SVXII Group

PIXEL98 Workshop
May 9, 1998

- Overview
- High-Density Interconnect Cable
- Long Cu-Kapton Cable
  - General Design
  - Special Features
- Summary

Overview

- The CDF SVXII Detector is a five-layer silicon strip detector. Each cylindrical barrel is divided into twelve wedges.
- Each wedge has at its outermost radius a port card. The port card receives electrical timing signals from the external DAQ electronics, and sends back data via optical fibers.
- The detector power and timing signals for a given wedge are carried on a single Cu-Kapton cable, called the Long Cu-Kapton cable.
- This cable connects between to the port card, and runs 6 feet out of the detector volume, where it connects to standard flat cables.

Cross Sectional View of Barrel End

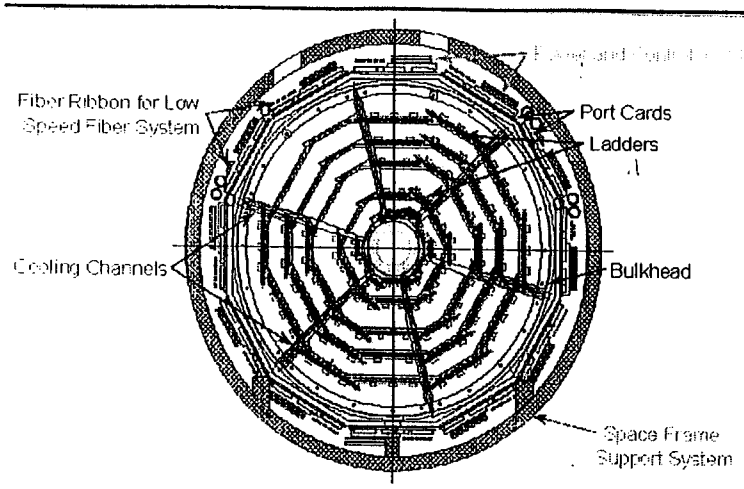

Slide 5 of 57

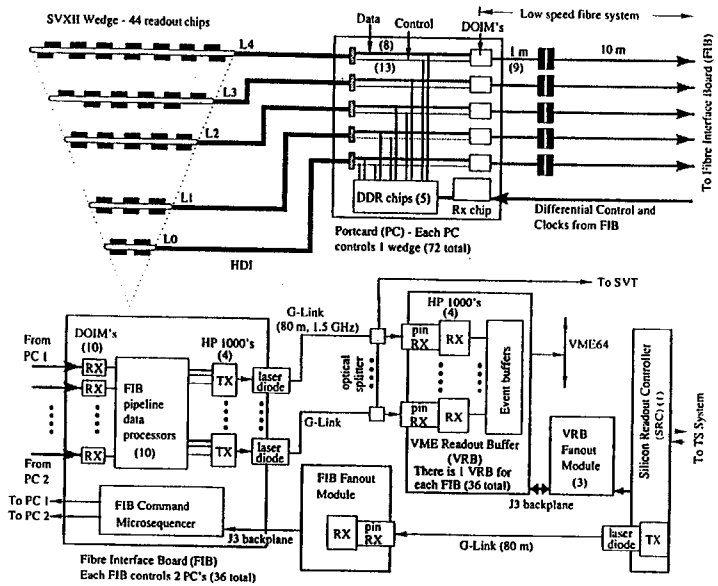

Figure 5: Schematic of the SVX II data acquistion system. The upper half shows the frontend readout mounted on or near the SVX II. The FIB system is in VME crates on the sides of the CDF detector, and the VRB system and SRC are in the counting room.

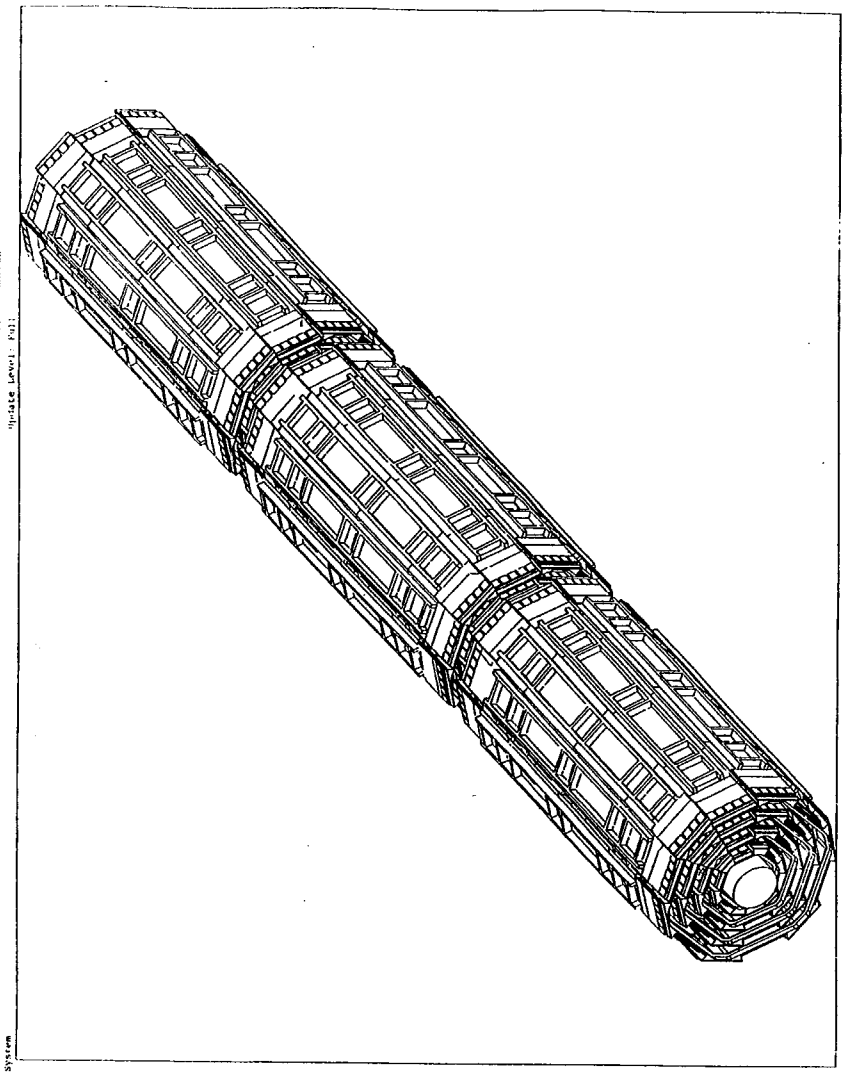

- **Each layer of a wedge has SVX3 custom readout chips, mounted on a hybrid. The port card connects to each of the 5 layers using a compact HDI cable.**

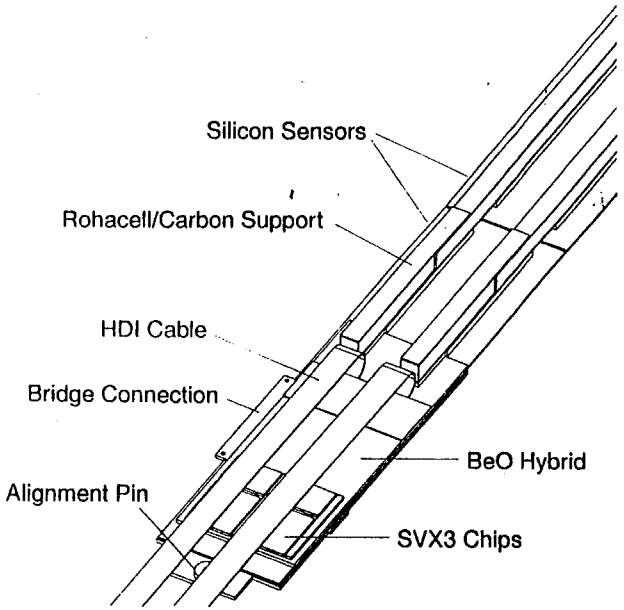

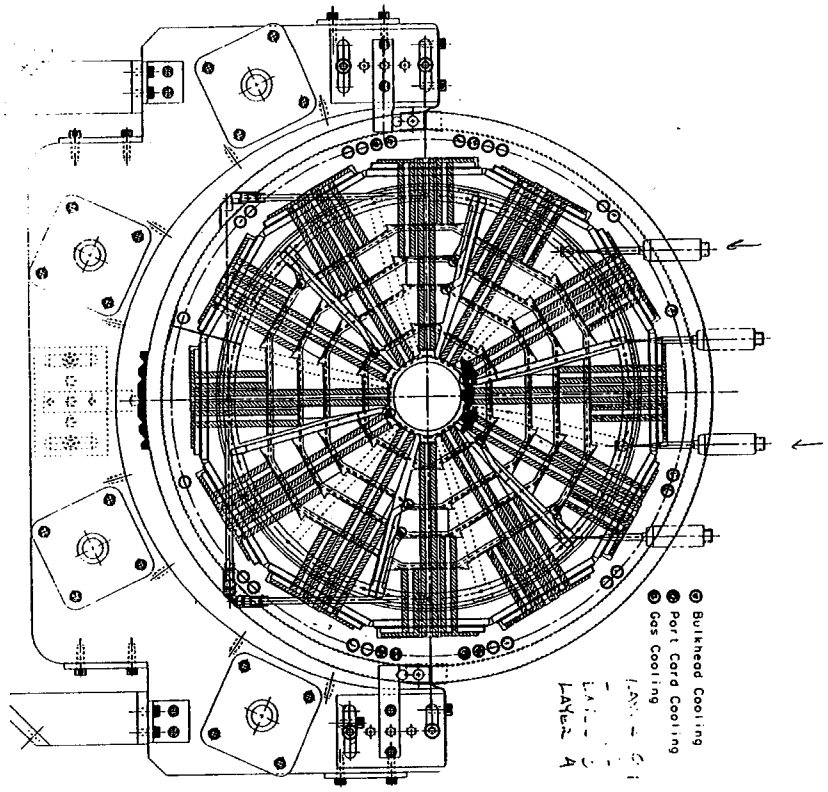

Figure 3: Schematic of an SVX II layer 0 half-ladder consisting of 2 silicon sensors. Electronics for the readout are mounted on the first sensor. The z-side SVX3 chips are on the underside and are not visible.

High-Density Interconnect (HDI) Cable

- Carries power and timing signals between port card and layer hybrids
- Tight space constraints demand high trace density and compact design

- Design/layout at University of New Mexico (with M. Gold, J. Behrendt, and M. Garcia-Sciveres(LBL))
- Prototypes fabricated by Dynaflex Technology, San Jose, CA.

Mark Bailey
PIXEL98 Workshop
May 9, 1998

HDI Cable General Design

- 1/2 oz./ft^2 copper on 2 mil Kapton
- Signal traces are 3 mil wide, with a 7 mil pitch, broad-side coupled (signal and its complement are on opposite sides of the Kapton)
  - (This is near the limit of most vendors' capabilities)
- Power is carried on discrete 34 AWG wires, soldered onto the cable
- Total size $9.9'' \times 1.1''$

Mark Bailey
PIXEL98 Workshop
May 9, 1998

HDI Cable
Special Features

- **Densely packed solder pad array: Holes are 5 mil in diameter on a 10 mil pad**
  - Most vendors can't meet such a tight tolerance
  - More easily done when pads are close together in a regular pattern
  - For single pads, usual tolerance is a 10 mil annular region about the hole
- **Accommodates Berg Electronics "zero insertion-force" connectors**
  - Teardrop transition from traces to pads
  - Tin plating on contact fingers

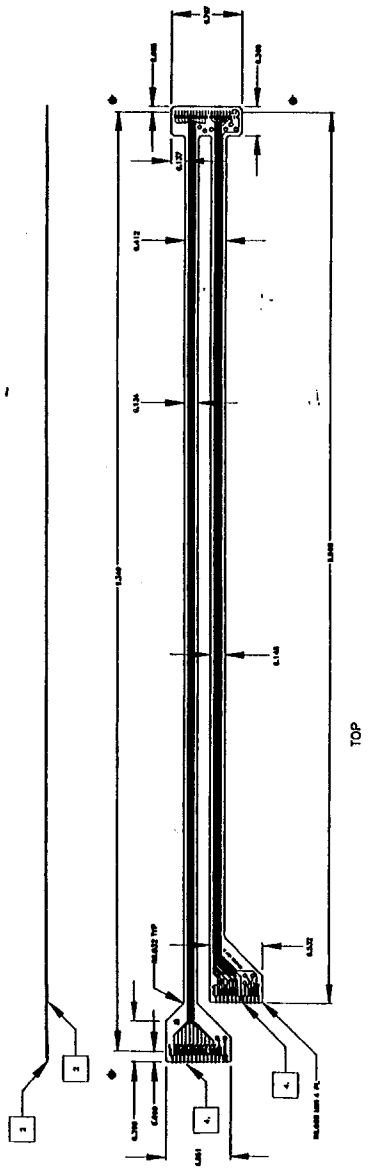

NOTES:
1. MATERIAL: BASE MATERIAL POLYIMIDE .002 THK. 1/2 OZ COPPER BOTH SIDES
2. PLACE BACKING MATERIAL OPPOSITE CONTACT FINGERS IAW BERG ELECTRONICS DWG NO 87768
3. COVERLAY 1.5 MIL PHOTO BOTH SIDES
4. HARD NICKEL/GOLD PLATE CONTACT FINGERS

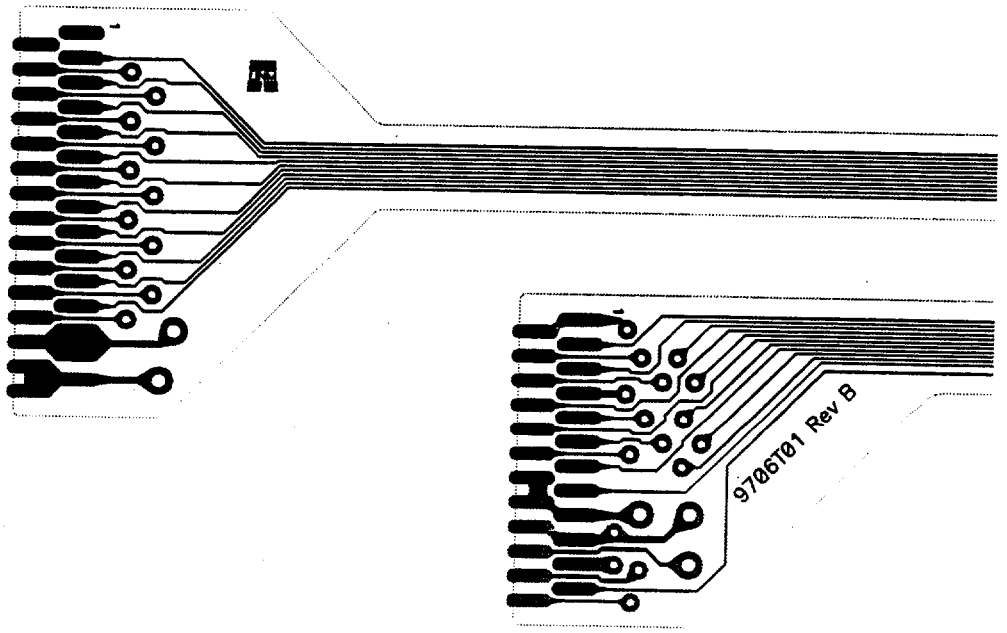
9706T01 Rev B

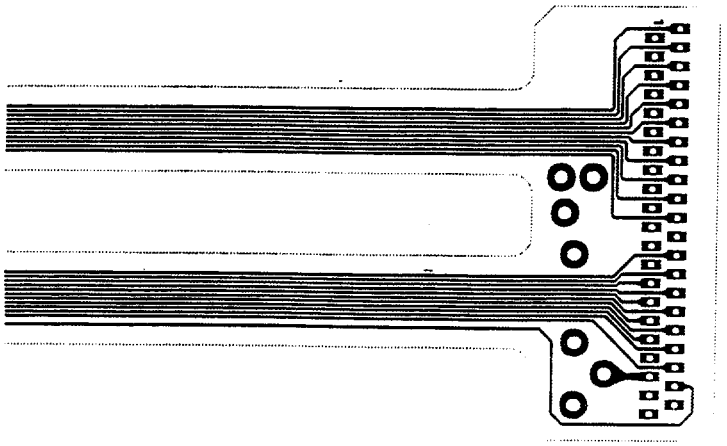

Long Cu-Kapton Cable

- Carries power and timing signals from standard flat cables outside the detector in to the port card, along the beamline near the interaction region
- Relatively low-mass Cu-Kapton solution was chosen to reduce multiple scattering in the region
- Also need to control voltage drop along the cable, and match the impedance of signal lines with the external flat cable

- Design/layout at Fermilab (with J. Anderson and J. Franzen)
- Prototypes fabricated by Speedy/Metro Circuits, Huntington Beach, CA

Mark Bailey
PIXEL98 Workshop
May 9, 1998

Long Cu-Kapton Cable General Design

- 1 oz./ft^2 copper on 5 mil Kapton
- Signal traces are 8 mil wide, with a 15 mil pitch, broad-side coupled, giving an impedance of 101Ω
- Power traces are opposite respective return lines, for low inductance
- Total size $6' \times 2.4''$

Mark Bailey
PIXEL98 Workshop
May 9, 1998

Long Cu-Kapton Cable Special Features

- **SIZE:**
  - Length greatly limits number of vendors available, and raises the cost
  - Many long cable vendors can etch on only one side
- **Signal trace width set to give $\sim 100\Omega$ impedance, well matched with standard flat cables**
- **Trace widths of power lines chosen to give a drop of less than 0.5 V across the length of the cable**
- **Cable mass averaged over phi is about 0.55% X_0**

TOP LAYER

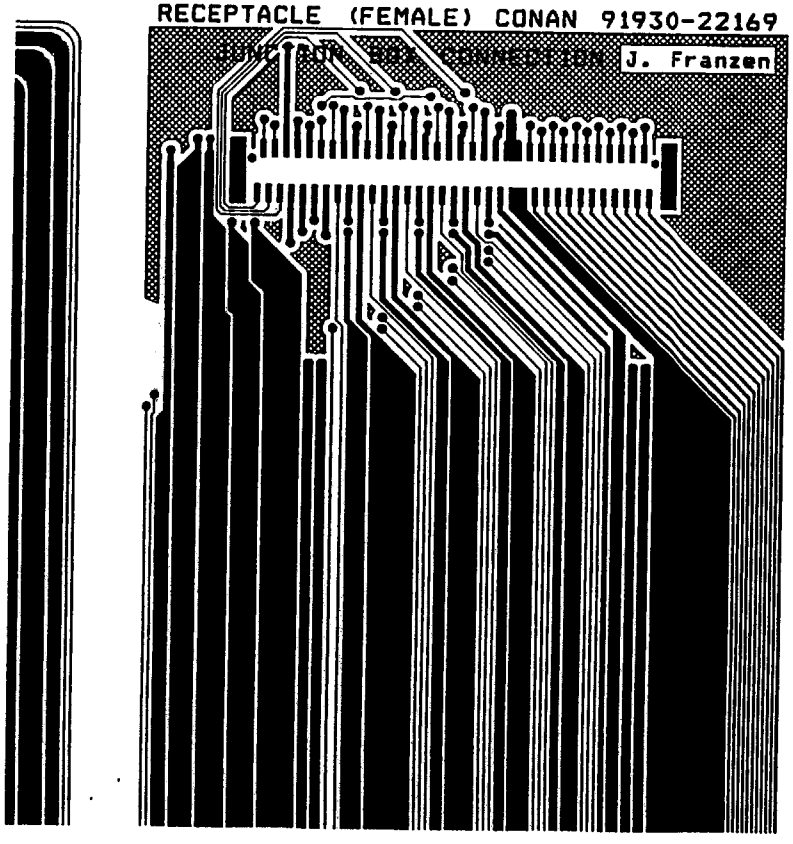

Mark Bailey
PIXEL98 Workshop
May 9, 1998

Long Cu-Kapton Cable Special Features

- Small prototype runs at reasonable cose aren't available for long cables
- Prototype uses a serpentine layout, which folds out to give full length. Might be a reasonable solution, but signal propagation and susceptibility for traces to break needs to be investigated
- Inaccessibility of the cable in this area precludes connecting several shorter cables together

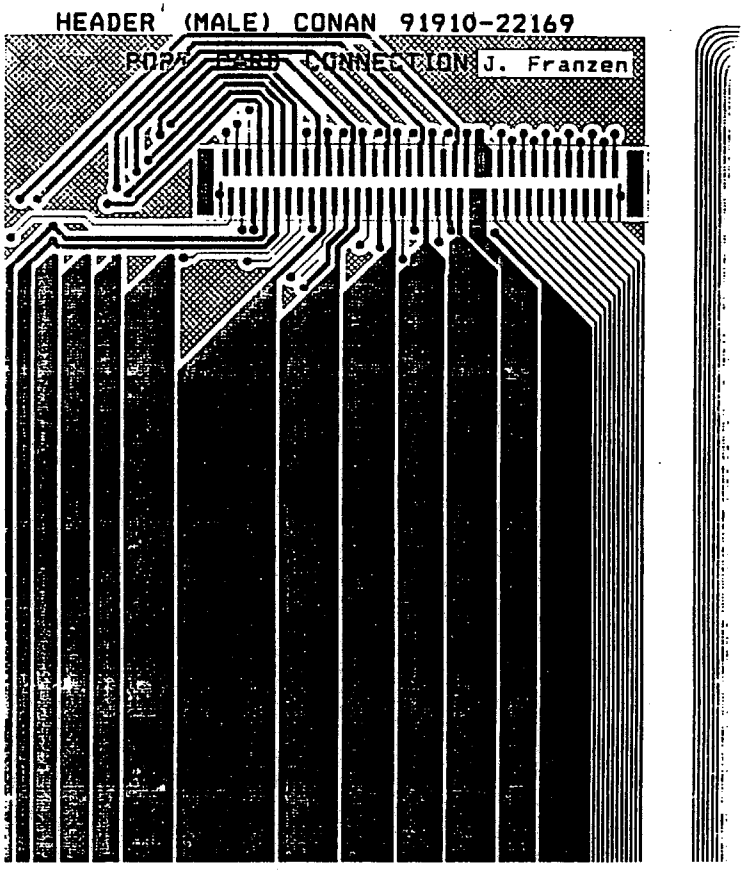

Summary

- The CDF SVXII group has exploited Cu-Kapton flexible circuit technology to provide two of its interconnection cables
- The HDI cable uses a small trace width size and dense solder pad array which are near the limits of most vendors' technical capabilities
- The Long Cu-Kapton cable tests another limit: the maximum circuit size available. Serpentine design might be a viable solution, which uses a circuit dimension more typical in the industry
- Cu-Kapton cable design properties and limitations should be considered at an early stage in the design of the components to which they are to be connected
- Fortunately, there are a large number of vendors with complementary capabilities. With some persistence, one can usually find one who can meet one's design requirements